BIROn - Birkbeck Institutional Research Online

1 **Ca isotope constraints on chemical weathering processes:**

2 **Evidence from headwater in the Changjiang River, China**

3

4 **Bei-Bei Chen [a], Si-Liang Li [a, b, *], Philip A.E. Pogge von Strandmann [c],**

5 **Jian Sun [d], Jun Zhong [a], Cai Li [a], Ting-Ting Ma [a], Sen Xu [a], Cong-Qiang**

6 **Liu [a]**

7

8 *a* Institute of Surface-Earth System Science, Tianjin University, Tianjin 300072,

9 China

10 *b* State Key Laboratory of Hydraulic Engineering Simulation and Safety, Tianjin

11 University, Tianjin 300072, China

12 *c* London Geochemistry and Isotope Centre (LOGIC), Institute of Earth and

13 Planetary Sciences, University College London and Birkbeck, University of

14 London, Gower Street, London WC1E 6BT, UK

15 *d* Key Laboratory of Deep-Earth Dynamics of Ministry of Natural Resources,

16 MNR Key Laboratory of Isotope Geology, Institute of Geology, Chinese

17 Academy of Geological Sciences, Beijing 100037, China

18

20 *Corresponding authors: Si-Liang Li

21 State Key Laboratory of Hydraulic Engineering Simulation and Safety,

22 Tianjin University 92# Wei-Jin Road, Nankai District

23 Tianjin 300072, China

24 Fax: (+86-22) 8737 0955

25 Email: Siliang.li@tju.edu.cn

26

Abstract

This study aims to clarify the relationship between chemical weathering of rocks and the carbon budget of rivers and to better understand the weathering mechanisms of plateau watersheds. We chose to study the Jinsha River, which originates from the Tibetan Plateau and also is in the upper reaches of the Changjiang River. Analysis of hydrochemistry, radiogenic strontium isotope and stable calcium isotopes were conducted of the Jinsha River water samples, which were collected along its mainstream and main tributaries in the summer. The results show that the water chemistry of the mainstream is dominated by evaporite weathering, which has a low $^{87}Sr/^{86}Sr$ (0.7098 to 0.7108) and wide range of Sr contents (2.70 to 9.35 μmol/L). In contrast, tributaries of the Jinsha River have higher $^{87}Sr/^{86}Sr$ (0.7090 to 0.7157) and lower Sr contents (~1μmol/L). Moreover, the Ca isotopic compositions in the mainstream (0.87-1.11‰) are heavier than the tributaries (0.68-0.88‰) and could not attribute to the conventional mixing of different sources. We suggest that secondary carbonate precipitation fractionates Ca isotopes in the Jinsha River, and fractionation factors are between 0.99935 and 0.99963. At least 66% of dissolved Ca is removed in the mainstream of the Jinsha River through secondary mineral precipitation, and the average value is ~35% in the tributaries. The results highlight that evaporite weathering results in more carbonate precipitation influencing Ca transportation and cycling in the riverine system constrained by stable Ca isotopic compositions and water chemistry.

1. Introduction

Calcium is the fifth most abundant element in the earth's crust and can migrate easily between major geochemical reservoirs at the Earth's surface (Rudnick and Gao, 2014; Tipper et al., 2016). As one of major components of rock and minerals, Ca is participant in many critical processes related to the co-evolution of earth and life, including carbon cycling, the evolution of marine chemical components and long-term climate change (Berner and Berner, 2012; Berner, 2003; Berner et al., 1983; Walker et al., 1981). Chemical weathering of rocks and minerals plays a key role in those processes, in which rocks and minerals react with dissolved acidic gases (such as CO_2 and SO_2) and water in the atmosphere, releasing dissolved metal ions and forming secondary minerals. Solutes are transported to the ocean through rivers, regulating the chemical balance of seawater and absorbing CO_2 in the atmosphere to bury them in the form of carbonate (Gaillardet et al., 1999; Schmitt et al., 2003; West et al., 2005; White and Blum, 1995). Other products of rock weathering, such as clay minerals, will be accumulated to the floodplain along the river, forming an important part of soil (Tipper et al., 2006; Torres et al., 2015; West et al., 2005).

Riverine input of Ca is a key component in the global Ca model, where

3

71 oceans impact climate through regulation of atmospheric CO_2 (Gaillardet et al.,

72 1999). The study of Ca fluxes and their isotopic compositions in rivers could

73 help understand whether Ca in the ocean is in equilibrium (DePaolo, 2004;

74 Schmitt et al., 2003; Tipper et al., 2010; Zhu and Macdougall, 1988). This also

75 determines whether the Ca isotopes can be used as an indicator for the study

76 of the paleo-ocean to explore paleo-sea surface temperature (SST) and its

77 corresponding P_{CO2}, which are closely related to long-term climate change

78 (DePaolo, 2004; Fantle, 2010, 2015; Fantle and DePaolo, 2005; Pogge von

79 Strandmann et al., 2013; Pogge von Strandmann et al., 2012; Rocha and

80 DePaolo, 2000). On the other hand, riverine Ca fluxes produced by rock

81 weathering are an important part of the ocean Ca budget, which has a

82 significant impact on the global carbon cycle together with the precipitation of

83 carbonate in the ocean (Schmitt, 2016; Tipper et al., 2016). Many studies have

84 focused on the behavior of Ca isotopes during rock weathering and material

85 transport by rivers (Cenki-Tok et al., 2009; Fantle and Tipper, 2014; Hindshaw

86 et al., 2013; Hindshaw et al., 2011; Jacobson et al., 2015; Lehn et al., 2017;

87 Marie-Laure Bagard et al., 2013; Marie-Laure Bagard et al., 2011; Moore et al.,

88 2013; Schmitt, 2016; Schmitt et al., 2003; Tipper et al., 2006; Tipper et al., 2010;

89 Tipper et al., 2008; Tipper et al., 2016; Wiegand and Schwendenmann, 2013).

90 Ca isotopes could not only trace the Ca cycle directly but also be a potential

91 tracer in mineral carbonation and the C cycle (Pogge von Strandmann et al.,

92 2019a).

Previous studies show that Ca isotopes in rivers may mainly controlled by different factors across different scales. For small rivers, a variety of factors result in changeable Ca isotopic compositions ($\delta^{44/40}$Ca) which exhibit a wide range from 0.27to 1.70‰. Ca isotopic compositions are not only controlled by mixing of different sources, such as lithology, underground water and soil water (Hindshaw et al., 2011; Jacobson et al., 2015; Jacobson and Holmden, 2008; Jacobson and Wasserburg, 2005), but also by secondary processes, such as the uptake of plants (Brazier et al., 2019; Cenki-Tok et al., 2009; Farkaš et al., 2011; Hindshaw et al., 2012; Holmden and Bélanger, 2010; Schmitt et al., 2017), the neoformation of secondary mineral phases (soil carbonates, travertines and Ca-bearing clays) (Hindshaw et al., 2013; Tipper et al., 2006) and the adsorption by clays (Brazier et al., 2019; Ockert et al., 2013). With regards to world rivers, although complex lithology and variable climate and vegetations result in different hydrochemistry and Sr isotopic compositions, the ratios of Ca isotopes are quite homogeneous (Schmitt, 2016). Samples collected at river mouths show small $\delta^{44/40}$Ca variations of 0.56‰, ranging from 0.69 to 1.25‰ with an average of 0.86‰ (Schmitt et al., 2003; Tipper et al., 2010; Zhu and Macdougall, 1988). The main controlling factors of Ca isotopes in world rivers are still controversial. Fantle and Tipper (2014) calculated the average Ca isotopic composition of carbonate and silicate as 0.6‰ and 0.94‰ respectively. Combined with the global riverine Ca flux, the mean theoretical Ca isotope ratio of the riverine flux is 0.630.69‰, which is lower than the measured value of

115 continental runoff (0.86 ± 0.06‰) (Tipper et al., 2016). Therefore, they

116 suggested that secondary processes, such as the plant uptake, secondary

117 mineral formation and clay adsorption, play an important role in the riverine Ca

118 isotopic composition. However, Jacobson et al. (2015) analyzed riverine Ca

119 isotope values in Iceland, and demonstrated that the dissolution of

120 hydrothermal calcite in basalt dominates the Ca isotopic ratios of river in Iceland.

121 They also suggested that conventional mixing processes stemming from

122 mineral dissolution dominates the Ca isotopic compositions of global rivers.

123 These studies suggested riverine Ca behavior relating with geological

124 characteristics were not well explored and the dominant factors controlling

125 riverine Ca isotopes still need to be further clarified.

126 Overall, the monitoring of Ca isotope behavior along rivers is still lacking

127 (Schmitt et al., 2003; Tipper et al., 2010; Zhu and Macdougall, 1988). Although

128 the factors affecting the Ca isotope value of rivers can be evaluated qualitatively,

129 some critical isotope signals may be overprinted (Hindshaw et al., 2013),

130 meaning that it is difficult to fully understand and interpret Ca isotope ratios.

131 Moreover, abundant previous studies focus on silicate weathering (Cenki-

132 Tok et al., 2009; Hindshaw et al., 2013; Hindshaw et al., 2011; Holmden and

133 Bélanger, 2010; Marie-Laure Bagard et al., 2013; Nielsen and DePaolo, 2013;

134 Schmitt et al., 2003; Wiegand and Schwendenmann, 2013), and several

135 researchers have studied the effect of sedimentary rocks weathering on carbon

136 budget (Gaillardet et al., 2018; Lehn et al., 2017; Moore et al., 2013; Tipper et

al., 2006; Tipper et al., 2008), but studies on evaporite weathering are very rare (Wang et al., 2018; Wellman and Wilson, 1965). As a common rock in the earth-surface, evaporites are often accompanied by sedimentary rocks, such as limestone, dolomite and mudstone. Although the total amount of evaporites is less than that of silicates and carbonates, it has great influence on water chemistry owing to its high solubility and fast dissolution rate (Wang et al., 2018; Wellman and Wilson, 1965). For example, the dissolution of gypsum releases a large amount of Ca into the water, which to a certain extent increases the absorption of CO_2 by the river and affects the overall carbon budget (Farkaš et al., 2007). Previous studies on the Ca isotopes of evaporites have been focused on evaporites from seafloor hydrothermal precipitation (Amini et al., 2008; Blättler and Higgins, 2014; Galy and France-Lanord, 1999; Hensley, 2006; Holmden, 2009) and several laboratory precipitation experiments of anhydrite (Harouaka et al., 2014; Hensley, 2006; Lemarchand et al., 2004), which were used to assess the impact of seafloor hydrothermal input on marine Ca isotopic compositions. However, evaluations of the influence of continental evaporite weathering on water chemistry and even Carbon budget are still rare (Jacobson and Holmden, 2008; Jacobson and Wasserburg, 2005; Russell et al., 1978).

In this study, we collected water samples from the mainstream and main tributaries of the upper Jinsha River. Water chemistry in the mainstream is mainly dominated by evaporates dissolution (Chetelat et al., 2008; Gaillardet et al., 1999; Noh et al., 2009; Wu et al., 2008; Zhao et al., 2019; Zhong, 2017).

159 Through analyzing data of hydrochemistry, Ca and Sr isotopes in the Jinsha

160 River Basin, the dominant factors controlling the calcium transportation of the

161 Jinsha River are evaluated, then the influence of evaporite weathering on

162 carbon transportation is assessed, which could lay a foundation for further

163 exploring the mechanism of solute transportation impacted by secondary

164 processes in the rivers origin from the Tibetan Plateau.

165

2. Regional setting

167 The Jinsha River Basin is located in the eastern Tibetan Plateau,

168 Southwest China. As the headwaters of the Changjiang River, the Jinsha River

169 originates at the end of the ice tongue of the Gladandong Mountains in the

170 middle of the Tanggula Mountains in Qinghai Province at an elevation of 6621

171 m. The source river of the Changjiang River is mainly composed of Dangqu

172 (south source), Tuotuo River (the main source) and Chumar River (north

173 source). They converge as the Tongtian River, which flowed southeast to accept

174 the Batang River near Yushu County, Qinghai Province, after which it is called

175 the Jinsha River (Su and Chen, 2016; Wu et al., 2011; Wu et al., 2009a; Wu et

176 al., 2008; Zhang et al., 2016; Zhao et al., 2019) (Fig. 1a). The Jinsha River has

177 a basin area of 473,640 km^2 with a mainstream river length of over 2316 km,

178 accounting for 2/3 of the length of the upper reaches of the Changjiang River

179 (Su and Chen, 2016). The upper, middle, and lower reaches of the river are

180 divided by Shigu and Panzhihua stations. Significant differences in topography

and geomorphology are observed in the Jinsha River Basin, leading to great differences in regional climate and water cycle processes in the upper, middle and lower reaches (Xie et al., 2018). The source region of the Jinsha River is located in the southeast of the Qinghai-Tibet Plateau, with an average altitude of more than 5000 m, showing typical plateau landscape where climate is cold and dry. Runoff of source river is mainly supplied by ice and snow melt water and permafrost, so that water cycle is significantly affected by air temperature. The upper reach of the Jinsha River is accompanied by significant topographic differences changing from plateau to typical dry-hot valley. Surrounded by mountains, external water vapor rarely enters, leading to rare precipitation and significant evaporation. The middle reaches of the Jinsha River flow between the deep canyons. The average annual precipitation increases from northwest to southeast, mostly ranging from 600 mm to 1000 mm, and reaches 1300mm in some areas. As to the lower reach of the Jinsha River, terrain changes from canyon to hilly and plain. The average annual precipitation is 600 - 1500 mm and in some areas more than 1800 mm, and the evaporation is small. The water cycle in this area is different from that in the upper and middle reaches on account of the great influence of human activity (Liu, 2016; Lu et al., 2016; Xie et al., 2018; Zhang et al., 2016; Zhang et al., 2018).

The upper and middle reaches of the Jinsha River were selected as our research area because of little anthropogenic impact (Zhao et al., 2019) (Fig. 1). Evaporites weathering significantly affect the Jinsha River mainstream

(Chetelat et al., 2008; Gaillardet et al., 1999; Noh et al., 2009; Zhao et al., 2019; Zhong, 2017). Mesozoic clastic rocks and evaporites are mainly exposed in the source area, and the research area in this study is mainly composed of Triassic low-grade metamorphic rocks, Paleozoic carbonate rocks and basalts, accompanied with scattered Mesozoic granitoids and Mesozoic ophiolitic mélanges along the upper reach valley (Wu et al., 2009a; Wu et al., 2008; Wu et al., 2013; Zhang et al., 2016; Zhao et al., 2019).

3.   Method

3.1 Water samples

Water samples were collected in June 2016, corresponding to the high flow season. Temperature, electrical conductivity and pH of the water samples were measured in the field. Alkalinity was determined by HCl titration. Water samples were filtered through 0.45 µm cellulose-acetate filters into a series of pre-cleaned HDPE bottles for analysis. Major cations (Ca, Mg, Na, K) and Si concentrations were measured by ICP-OES with a precision better than 5% (2 δ_{mean}). Anions (Cl, SO_4) were determined by ionic chromatography Dionex 90 with a precision of 5%. The values of partial pressure of CO_2 (P_{CO2}) and calcite saturation index (CSI) were calculated by the programmer PhreeqC (Parkhurst and Appelo, 1999).

3.2 Sample preparation for isotopic analysis

Both Ca and Sr are recovered together from the AG50 X12 columns. Because Ca is isotopically fractionated by this resin, quantitative recovery is necessary. River samples were dried down and re-dissolved in 1ml ultrapure HNO_3 on a hot plate at 120℃ for 24 h They were then dried and cooled down to room temperature, and then re-dissolved in 1ml ultrapure HNO_3 with 100 μL H_2O_2 on a hot plate at 90℃ for 1 h to remove organic matter. Note that then these samples also need to be dried down no higher than 90℃ to prevent H_2O_2 from exploding when heated. After that, they were re-dissolved in 1 ml ultrapure HCl for 1 h and then dried down at 120℃. They were finally dried and re-dissolved in 1ml 2N HCl for chemical purification.

The protocols for Ca and Sr separation in this study are modified from (Chu et al., 2006; Nan et al., 2015; Owen et al., 2016). The column used a 30mL Teflon® micro-column with 6.4mm ID × 9.6mm OD (Savillex®), filled with 2mL AG50W-X12 resin (200-400 mesh, Bio-Rad, USA). Columns were precleaned with 20mL 6 mol/L HNO3 and 3mL 6 mol/L HCl, and then conditioned with 3mL 18.2 MΩ H_2O, before sample loading.

1mL sample solutions containing ~100ug Ca were loaded and 19mL 2 mol/L HCl was used to elute the matrix elements including Na, Mg, K, Fe and Mn. Ca was then collected with 18mL 2 mol/L HCl. Following Ca collection, 2mL 3 mol/L HCl was used to elute the tailing of trace Ca. Sr was then collected with 10mL 3 mol/L HCl. Both 2mL aliquots before and after the Ca-cut were collected

246 and measured for their Ca contents to test whether the Ca elution curve drifted

247 during the chromatographic process. After the column protocols, Ca and Sr

248 collections were dried and dissolved in concentrated HNO_3, evaporated to

249 dryness three times, and finally dissolved in 0.3 mol/L HNO_3 before isotope

250 analysis (Sun et al., 2019).

251   Ca isotopic analysis was undertaken using the Nu Instruments MC-ICPMS

252 at the Laboratory of Isotope Geology, Institute of Geology, Chinese Academy of

253 Geological Sciences, Beijing, China. Isotopes of ^{42}Ca, ^{43}Ca and ^{44}Ca were

254 measured at low-resolution. The standard-sample bracketing (SSB) approach

255 (Belshaw et al., 2000) was used to correct the mass discrimination, using NIST

256 915a or NIST 915b as the reference standard, and with sample and standard

257 solutions being matched to give ^{42}Ca intensities with differences less than 10%.

258 All samples were normally repeatedly analyzed for 3~5 times for one session.

259 The external precision of Ca isotope ratios ($^{44}Ca/^{42}Ca$) during the measuring

260 period is better than 0.07‰ (2SD) based on the repeated measurements of

261 standard NIST 915b. Calcium isotope values can be converted using:

262 $$\delta^{44/40}Ca = 2.048 \times \delta^{44/42}Ca \quad \text{(Heuser et al., 2016)}. \qquad (1)$$

263 Data in this study are presented as $\delta^{44/40}Ca$ relative to the NIST SRM915a

264 standard:

265 $$\delta^{44/40}Ca \ (‰) = 1000\left\{\frac{\left(^{44}Ca/^{40}Ca\right)_{sample}}{\left(^{44}Ca/^{40}Ca\right)_{SRM\,915a}} - 1\right\} \qquad (2)$$

266   Sr isotopic analysis was undertaken at the Institute of Surface-Earth

267 System Science, Tianjin University. The Sr isotope composition were measured

268 using MC-ICPMS and the instrumental mass fractionation was corrected by

269 internally normalizing the $^{87}Sr/^{86}Sr$ ratio to 0.1194. The average $^{87}Sr/^{86}Sr$ ratio

270 for NBS 987 was 0.710271 ± 0.000030 (2SD, n = 34).

271

272 **4. Results**

273 **4.1 Water chemistry**

274 The pH of the river water samples ranges from 8.06 to 8.66 with an average

275 of 8.35 (Table 1). The temperature of river water is 12.7 to 22.4℃ with an

276 average of 16.3℃. The chemical compositions for the Jinsha River waters vary

277 significantly (Chetelat et al., 2008; Gaillardet et al., 1999; Noh et al., 2009; Wu

278 et al., 2008; Zhao et al., 2019; Zhong, 2017), with the total dissolved solids

279 (TDS = Ca + Mg + Na + K + Cl + HCO_3 +SO_4 + SiO_2) ranging from 88 to 689

280 mg/L. The range of TDS values in the mainstream (301~689 mg/L) is higher

281 than tributaries' values (88~268 mg/L), and decrease from the upper reach to

282 the lower reach. The total cationic charges (TZ^+ =2*Ca + 2*Mg + Na + K) vary

283 dramatically ranging from 1130 μeq/L to 10,120 μeq/L. Ca^{2+} and Mg^{2+} are the

284 dominant cations in tributaries accounting for 59-96% of the total cationic

285 budget. In the mainstream, Na^+ is the dominant cation, accounting for 37-56%

286 for the total cationic budget. Besides, the dominant anions are HCO_3^- and Cl^- in

287 the main river water. Cl^- value of the mainstream samples gradually decrease

288 from upstream to downstream, HCO_3^- in tributaries show large variations and is

13

the dominant anion. Ca/Na ratios of the main river ranging from 0.24 to 0.59, which are lower than that of tributaries ranging from 4.50 to 11.39. Similarly, the range of Mg/Na ratios of mainstream is from 0.16 to 0.29 while that of tributaries is from 1.61 to 3.54.

In addition, to evaluate the calcite saturation state for river waters, calcite saturation indices (CSI) were calculated based on alkalinity, pH, temperature and ionic strength using the PHREEQC program (Parkhurst and Appelo, 1999). Results show that nearly all the Jinsha river waters are supersaturated for calcite (Table 2).

4.2 Strontium and its isotopic composition in the Jinsha River

The $^{87}Sr/^{86}Sr$ ratios and Sr concentrations of waters from the Jinsha River Basin are given in Table 1. The range of $^{87}Sr/^{86}Sr$ in the mainstream is similar to source rivers (Fig. 2) (Noh et al., 2009; Wu et al., 2009a; Zhao et al., 2003). Moreover, the median value of the source rivers is similar to that of the main stream and tributaries of the Jinsha River, which are close to 0.7100. However, the $^{87}Sr/^{86}Sr$ range of the Jinsha River sediments (JS sediment) is 0.7110 - 0.7147 (Wu et al., 2009b), which is higher than that of the source area, the tributaries and mainstream of the Jinsha River.

The mainstream of the Jinsha River (JS mainstream) has low variation in $^{87}Sr/^{86}Sr$ ratios with a narrow range of 0.7098 to 0.7108 and an average value of 0.7105, but shows significant changes in Sr contents from 2.70 μmol/L to

14

311 9.35 μmol/L with a general decrease from the upper reach to lower reaches

312 (Table 1, Fig. 3a). However, Sr contents of tributaries are almost constant

313 (~1μmol/L). $^{87}Sr/^{86}Sr$ ratios of the tributaries have a wider range, from 0.7090

314 to 0.7157 with an average of 0.7121 (Table 1; Fig. 3a).

315 Moreover, 1/Sr shows the strong positive correlation with Si/TZ$^+$ (Fig. 3b),

316 which implies a trend of mixing endmembers. Low 1/Sr and Si/TZ$^+$ signatures

317 in the waters could be related to carbonate and/or evaporite weathering in the

318 Jinsha River Basin. Moreover, silicate weathering will lead to high 1/Sr and

319 Si/TZ$^+$ signature in the waters. While the main stream also shows a simple

320 mixing relationship when plotting Sr isotopes against 1/Sr, the tributaries do not

321 have such a clear relationship (Fig. 3a), suggesting additional endmember

322 contributions.

323

324 **4.3 Ca isotopic compositions of the Jinsha River waters and gypsums**

325 The $\delta^{44/40}Ca$ of the dissolved load in the Jinsha River ranges from 0.68‰

326 to 1.11‰ with an average of 0.87‰, within the range of other large global

327 rivers (0.42-1.62‰) (Schmitt et al., 2003; Tipper et al., 2006; Zhu and

328 Macdougall, 1988).

329 The highest $\delta^{44/40}Ca$ value (1.11‰) is observed in the upstream reach of

330 the main stream (JS-1) and the lowest value (0.68‰) in a tributary in the upper

331 reach (JS-9). There is no systematic change trend of $\delta^{44/40}Ca$ from upstream

332 to downstream. In general, the mainstream generally has a higher $\delta^{44/40}Ca$

than the tributaries. Furthermore, $\delta^{44/40}Ca$ values have a significant positive

relationship with SO_4/Ca (Fig. 4a), and a slight negative correlation with Si/Ca

(Fig. 4b).

Moreover, rivers draining different lithological sources show a considerable

spread in Ca isotopic compositions based on literature compilations of data (Fig.

5). As a regional river originating from the Tibetan Plateau, the Jinsha River has

the same Ca isotopic range as rivers from the High Himalayan Crystalline

Series (HHCS) (0.69-0.92‰), which is lower than some Ca isotopic values in

rivers draining dolostone from Lesser Himalayan Series (LHS) (0.99-1.41‰),

but higher than some values in rivers draining limestone from Tethyan

Sedimentary Series (TSS) (0.50-1.30‰) (Tipper et al., 2008). The $\delta^{44/40}Ca$

values of the Jinsha River are also consistent with greywacke-draining rivers

from the Southern Alps, New Zealand (0.50-1.40‰) (Moore et al., 2013; Pogge

von Strandmann et al., 2019b). When compared with other small monolithologic

river catchments, the Ca isotopic composition of the Jinsha River is lower than

rivers draining granite in La Ronge (1.16-1.33‰) (Holmden and Bélanger, 2010)

and parts of the $\delta^{44/40}Ca$ values in basaltic rivers from Iceland (0.95-1.37‰)

(Hindshaw et al., 2013; Jacobson et al., 2015). Moreover, the $\delta^{44/40}Ca$ values

of the Jinsha River are higher than that in rivers draining granite in Exmoor

(0.50-0.99‰) (Chu et al., 2006) and Strengbach (0.27-0.86‰) (Schmitt et al.,

2003).

As a Ca-bearing mineral, gypsum, which is distributed widely in the source

area of the Changjiang River (Fig. 1a), is an important endmember for river

dissolved Ca. Five gypsum samples, collected from the source area of the

Changjiang River, show variable $\delta^{44/40}$Ca values from 0.24‰ to 0.95‰ with

an average of 0.61‰ (Table1). Among them, two gypsum samples collected

near the Dangqu River (G1 in Fig. 1a) have lower $\delta^{44/40}$Ca values (0.24-

0.27‰). Other three gypsum samples collected near the Tuotuo River (G2 and

G3 in Fig. 1a) have higher $\delta^{44/40}$Ca values (0.80-0.95‰).

5. Discussion

5.1 Sources of dissolved calcium in the Jinsha River

In the Jinsha River basin, potential sources of dissolved Ca are rain water

and dissolution of evaporite, silicate and carbonate. And the Ca budget

equation of the Jinsha River can be written as follows:

$$\left(Ca\right)_{river} = \left(Ca\right)_{rain} + \left(Ca\right)_{eva} + \left(Ca\right)_{sil} + \left(Ca\right)_{cab} \tag{3}$$

5.1.1 Atmospheric input

Sample JS-6 has the lowest chloride concentration of 5.8 μmol/L in all river

waters, which is consistent with the Cl concentration of local long-term

precipitation (0.9-32.7μmol/L) (Zhang et al., 2012) and also similar to that of

rain water in the Gula area at the middle reach of the Jinsha River (7.9 μmol/L)

(Zhao et al., 2019). Atmospheric input was corrected, assuming that the sample

with the lowest chloride concentration (JS-6) obtained its dissolved Cl

exclusively from rain water. Elemental ratios in precipitation from (Zhang et al.,

377 2012) were used to calculate the concentrations of other major ions (Ca, Mg,

378 Na, K) in rain water. Rain percentages (P_{rain}) are calculated by:

379 $$P_{rain} = \sum cation_{rain} \big/ \sum cation_{river} \qquad (4)$$

380 $$\sum cation_{rain} = Ca_{rain} + Mg_{rain} + Na_{rain} + K_{rain} \qquad (5)$$

381 Results are shown in Table 3. Cations from atmospheric sources account

382 for <5% of total riverine cations. In addition, the long term average Ca/Cl molar

383 ratio in rain waters is 4.34 (Zhang et al., 2012), and the Ca concentration of rain

384 water is 25.2 μmol/L, then the proportion of Ca derived from rain water to the

385 total of riverine Ca is 2-6%. Previous studies suggested $\delta^{44/40}$Ca values of rain

386 water ranging from -0.34 to 1.30‰ with an average value of 0.70 $\pm$ 0.16‰

387 (Han et al., 2019; Schmitt, 2016). The corrected riverine $\delta^{44/40}$Ca are elevated

388 by less than 0.08‰ or lowered by less than 0.02‰, within the long term

389 external precision ($\pm$0.14‰). Therefore, atmospheric precipitation has little

390 effect on riverine Ca isotopes.

391 **5.1.2 Rock weathering**

392 Based on the lithological distribution in the Jinsha River basin (Fig. 1a.),

393 silicate 1 (plutonic acid rock), silicate 2 (basaltic volcanic rock), carbonate, and

394 evaporite were chosen as the four main end-members. Meanwhile, strontium

395 isotopes suggest that water chemistry could be controlled by evaporite and

396 silicate as well as carbonate dissolution in agreement with the previous study

397 (Wu et al., 2011). From upstream to downstream of the Jinsha River, owing to

398 the increasing weathering input from silicates, concentration of dissolved Si in

18

both mainstream and tributaries increases, which is generally contrary to the decreasing Ca and SO_4 concentration (Fig. 6). However, there is no systemic change of $\delta^{44/40}Ca$ along the river. Hence, the Ca isotopic composition of the Jinsha River is not fully controlled by simple mixing between Ca signals of different rock end-members.

The Ca contribution of different rock sources could be calculated by an forward method (Chetelat et al., 2008). Na from silicates of Jinsha tributaries can be obtained by equation as follows:

$$\left(Na\right)_{sil} = \left(Na\right)_{river}^{*} - \left(Cl\right)_{river}^{*} \tag{6}$$

Where $(Na)_{sil}$ represents Na from silicate, and $(Na)^{*}_{river}$ and $(Cl)^{*}_{river}$ are dissolved Na and Cl in river collected from rain water. However, due to the diverse composition of evaporites (halite, mirabilites, sylvites, borates and sodium carbonate) in the salt lakes near the source area of the Jinsha River (Yu and Tang, 1980), Na from silicates of Jinsha mainstream cannot be obtained based on Eq. (6). A substitute method from (Wu et al., 2008) is conducted to obtain $(Na)_{sil}$ of mainstream. Assuming that the mainstream and its adjacent tributary have the similar dissolved $(Na)_{sil}$/Si ratio, then

$$\left(Na\right)_{sil-m} = \left(\left(Na\right)_{sil-t} / \left(Si\right)_{t}\right) \times \left(Si\right)_{m} \tag{7}$$

Where $(Na)_{sil-m}$ and $(Na)_{sil-t}$ are Na from silicate in Jinsha mainstream and tributaries, and $(Si)_{t}$ and $(Si)_{m}$ represent dissolved Si from Jinsha mainstream and tributaries. Then, dissolved Ca from silicate can be acquired as follows:

$$\left(Ca\right)_{sil} = \left(Na\right)_{sil} \times \left(Ca/Na\right)_{sil} \tag{8}$$

421   Where $(Ca)_{sil}$ represents the dissolved Ca from silicate, and $(Ca/Na)_{sil}$

422   represents the Ca/Na ratio of silicate widely distributed in the Jinsha river basin.

423   Here 0.49 ± 0.3 was used as the value of $(Ca/Na)_{sil}$, which is consistent with

424   the data of the silicate fraction of sediments in the Jinsha River (Wu et al.,

425   2009a). Calculated by Eq. (8), silicate weathering contributes 4-12 % of the

426   riverine Ca; including an uncertainty of 50% (Wu et al., 2009a), this propagates

427   to a 2-24% silicate contribution.

428   Assuming $(Ca/SO_4)_{eva}$ (the Ca/SO_4 ratio of evaporites in source area) is

429   0.95, which is equal to Ca/SO_4 ratios of source rivers (Tuotuo River and

430   Chumaer River) (Wu et al., 2009a), evaporite dissolution contributes 45-81% of

431   dissolved Ca to the Jinsha mainstream and 1-41% to the tributaries. Because

432   mirabilites are abundant in saline lakes near the source of the Jinsha River (Yu

433   and Tang, 1980), pyrite oxidation and sulphuric acid weathering (Chetelat et al.,

434   2008) also can affect the concentration of dissolved SO_4 in the Jinsha River.

435   The calculated $(Ca)_{eva}$ is the upper limit of evaporite Ca that can be obtained.

436   Through the budget equation (3) of Ca, the contribution of Ca from carbonate

437   weathering ranges from 6 to 43% in the mainstream and 47 to 88% in the

438   tributaries.

439   In addition, the initial Ca isotopic composition ($\delta^{44/40}Ca_0$) of the Jinsha River

440   water resulting from mixing of different rock sources could be calculated based

441   on a simple mixing equation as follows:

442    $$\delta^{44/40}Ca_0 = \sum_i \delta^{44/40}Ca_i \times \gamma_i^{Ca} \tag{9}$$

443 Where $\delta^{44/40}Ca_i$ represents the Calcium isotopic composition of source i, and

444 γ_i^{Ca} is the mixing proportion of Ca of each source *i* (evaporite, silicate 1, silicate

445 2 and carbonate) contributing to the dissolved load. Fantle and Tipper (2014)

446 compiled over 70 published Ca isotope studies, and obtained that the average

447 values of silicates and carbonates are 0.94‰ and 0.60‰, respectively. Thus,

448 0.94‰ was chosen as the $\delta^{44/40}Ca$ of the silicate endmember in this study.

449 Previous study (Tipper et al., 2006) suggested that the stable Ca isotope

450 composition of limestone in the Tibetan Plateau is 0.61‰, which is close to the

451 average value of worldwide carbonate (0.60‰), and also consistent with the

452 average value of sedimentary rocks of 0.64 ± 0.09‰ (2σmean; N=78) (Ewing

453 et al., 2008; Holmden, 2009; Jacobson and Holmden, 2008; Ludwik Halicz,

454 1999; Moore et al., 2013; Tipper et al., 2006; Tipper et al., 2008). Therefore,

455 0.61‰ was chosen as the carbonate endmember in this study. Moreover, we

456 suggest the average value of our gypsum samples (0.61‰) as the $\delta^{44/40}Ca$

457 value of the evaporite endmember, which is not only within the range of gypsum

458 data reported by Hensley (2006) (-0.52‰ to 1.68‰), but also similar to the

459 average $\delta^{44/40}Ca$ of anhydrites (0.65‰) suggested by other studies (Amini et

460 al., 2008; Holmden, 2009; Jacobson and Holmden, 2008).

461   Based on a conventional mixing model (Eq. (9)), the Jinsha River water

462 has a similar theoretical initial $\delta^{44/40}Ca$ value of 0.64‰, which is lower than

463 most of the measured values of the Jinsha River. In addition, a negative

464 correlation between $\delta^{44/40}Ca$ values and Si/Ca (Fig .4a) also conflicts with the

conventional mixing model. Hence, Ca isotopes must be fractionated in the Jinsha River.

5.2 Potential calcium isotope fractionation processes

5.2.1 Vegetable growth

Plants preferentially uptake lighter Ca isotopes, resulting in heavier Ca isotope in the remaining soil solutions. These will therefore elevate riverine Ca isotopes by mixing with river water (Cenki-Tok et al., 2009; Holmden and Bélanger, 2010; Schmitt et al., 2017).

The topography of the middle and upper sections of the Jinsha River basin is mainly dry and hot valleys with a slow growth rate of plants and low microbial activity in the soil (Liu, 2016). The Normalized Difference Vegetation Index (NDVI) was used to quantify the density of plant growth in the Jinsha River watershed (Table 1). Results show that there is no significant relationship between NDVI and the $\delta^{44/40}$Ca values of tributaries, implying that the Ca isotopic signal caused by plant growth may be overprinted by other signals, or its signal is too dilute to elevate the $\delta^{44/40}$Ca values of regional or global scale rivers significantly. Therefore, the effect of plant growth on riverine isotopes may need to be further constrained through tracing the Ca isotopic composition of the Jinsha River in space and time.

5.2.2 Mineral dissolution

Mg stable isotope fractionation has been shown to occur not only during

22

precipitation, but also during the congruent dissolution of magnesite (Pearce et al., 2012). There is also recent evidence that Ca isotopes can behave in the same way, i.e. exhibiting isotope fractionation during dissolution of calcite, and also at equilibrium (or dynamic equilibrium) (Oelkers et al., 2019). However, studies on Ca isotope fractionation between silicate minerals and corresponding fluids during water-rock interaction suggested that congruent dissolution of granite minerals at low temperature does not fractionate Ca isotopes (Cobert et al., 2011; Hindshaw et al., 2011; Ryu et al., 2011). From the above, dissolution of silicate rocks along the Jinsha River are not expected to cause significant Ca isotope fractionation.

5.2.3 Clay formation and adsorption

In the Jinsha River basin, similar clay mineral types exist between tributaries and the main stream (Zhao et al., 2019), illite and chlorite constitute the main part of the clay minerals in the suspended matter and sediments, followed by montmorillonite and kaolinite (Ding et al., 2013; Wu et al., 2011; Zhao et al., 2019). And the relative content of illite is 10 times higher than that of montmorillonite (Wu et al., 2011). This is also consistent with results of previous analyses of clay minerals in surface sediments of the whole Changjiang River basin (He et al., 2011).

It is hard to constrain the type and amount of the neoformed clay mineral directly. Fortunately, regional climate is linked to clay formation. For instance, illite and chlorite are always formed in dry-cold areas, such as the Changjiang

509 source area. In contrast, dry and hot environments, like the upper reaches of

510 the Jinsha River, are conducive to the formation of montmorillonite (He et al.,

511 2011). From upstream to downstream, the climate of the Jinsha river catchment

512 changes from dry-cold to dry-hot climate (Fig. 7). However, illite and chlorite are

513 also primary components of clay minerals in sediment and suspended matters

514 of rivers under dry-hot condition (from JS-3 to JS-16 in Fig.7). Combined with

515 the topographical conditions, one of the possible reasons is that pre-weathered

516 material in the dry-cold plateau is being eroded and transported, which is also

517 consistent with the unsaturated state of illite and chlorite in the Jinsha river

518 water (Table 2). Although the precise location of the formation of clay minerals

519 in rivers is still debated (i.e., soil solutions and/or river particulate material), the

520 saturation indices of clay minerals in river water can reflect the soil water to a

521 degree because of the connectivity between the river and soil solution. Kaolinite

522 and montmorillonite are supersaturated in the Jinsha river water, combined with

523 dry and hot climate condition, part of them are neoformed in the upper reaches

524 of the Jinsha River (from JS-3 to JS-16 in Fig. 7). However, riverine $\delta^{44/40}$Ca

525 show no systemic change with climate along the riverside. Therefore, the

526 influence of neoformed clay minerals on riverine Ca isotopic composition is

527 minor, assuming that environmental conditions are key in clay mineral formation

528 (Gislason et al., 1996; Stefánsson and Gíslason, 2001).

529   Previous studies suggested light Ca isotopes are preferentially adsorbed

530 to clays, and the degree of isotopic fractionation depends on types of clay

minerals and their grain sizes (Brazier et al., 2019; Ockert et al., 2013). Recent Ca isotope adsorption experiments show that no significant isotopic fractionation occurs when Ca isotopes are adsorbed by kaolinite (Brazier et al., 2019). This is inconsistent with results from Gussone and Dietzel (2016), who suggested that Ca isotope could be adsorbed strongly onto kaolinite accompanied with $\Delta^{44/40}Ca_{ads-fluid}$ ranging from -1.2~-3.0‰. Due to its fine grain size (<10 μm), newly formed K-mica may also preferentially adsorb light Ca isotopes, resulting in a positive apparent isotopic fractionation between 0.1‰ and 0.28‰ in the residual solution (Brazier et al., 2019). Moreover, Ca isotopes adsorbed onto illite cause $\Delta^{44/40}Ca_{ads-fluid}$ ranging from -0.5 to -1.2‰ (Gussone and Dietzel, 2016), and Ca adsorption and the related isotopic fractionation are thought to be fully reversible (Brazier et al., 2019). In the Jinsha River waters, k-mica, kaolinite and montmorillonite are supersaturated, and negative correlations were obtained between their saturation index and $\delta^{44/40}Ca$ values in tributaries. This conflicts with results from laboratory experiments, which suggest that adsorption by clay minerals leads to heavier $\delta^{44/40}Ca$ in residual solutions and there should be a positive correlation between the saturation index of clay minerals and riverine $\delta^{44/40}Ca$ values. Therefore, the influence of clay mineral adsorption on Ca isotopic compositions of Jinsha tributaries is minor. In addition, although quantitative evaluation of the impact of Ca adsorption on riverine $\delta^{44/40}Ca$ is difficult, Ca flux sorption to the exchangeable fraction may be restrained by excess Na resulting from evaporite dissolution in

553   the mainstream of the Jinsha River, since it also could impact the $\delta^{44/40}Ca$

554   values if Na is replaced by lighter Ca isotopes preferentially (Jacobson and

555   Holmden, 2008; Ockert et al., 2013).

5.2.4 Carbonate precipitation

557   Calcium isotopes are fractionated during authigenic carbonate

558   precipitation from aqueous solutions (Gussone and Dietzel, 2016), which

559   preferentially takes light Ca isotopes into the solid (Blättler et al., 2015; Böhm

560   et al., 2012; Gussone et al., 2003; Gussone et al., 2011; Henderson et al., 2006;

561   Holmden, 2009; Jacobson and Holmden, 2008; Nielsen and DePaolo, 2013;

562   Oehlerich et al., 2015; Steuber and Buhl, 2006; Teichert et al., 2005; Tipper et

563   al., 2006; Wang et al., 2012; Wang et al., 2013), consistent with the fractionation

564   displayed by laboratory precipitation experiments of calcite (Gussone et al.,

565   2003; Gussone et al., 2011; Lemarchand et al., 2004; Tang et al., 2008; Tang

566   et al., 2012). If secondary Ca-bearing minerals are causing the observed

567   fractionation of Ca isotopes in the Jinsha River, the fractionation factor in this

568   process can be calculated (Hindshaw et al., 2013).

569   The correlation between metal isotopic compositions ($\delta^{44/40}Ca$, $\delta^{26}Mg$)

570   and saturation indices of carbonates could indicate carbonates precipitation

571   (Fan et al., 2016; Hindshaw et al., 2013; Moore et al., 2013; Pogge von

572   Strandmann et al., 2019a; Pogge von Strandmann et al., 2019b; Pogge von

573   Strandmann et al., 2019c; Tipper et al., 2008).The positive relationship between

574   riverine $\delta^{44/40}Ca$ values with CSI and Sr/Ca ratios (Fig. 8a and b), implies that

575 carbonates precipitation may elevate the Ca isotopic compositions of the Jinsha

576 River waters. f_{Ca} represents the fraction of Ca still in solution. If f_{Ca} equals to 1,

577 there will be no Ca incorporated into secondary minerals after its initial

578 dissolution. In contrast, all Ca from primary mineral dissolution will precipitate

579 as secondary minerals when f_{Ca} has a value of 0. Assuming that the release of

580 Ca and Na from bed rocks is congruent, f_{Ca} can be calculated as below:

581
$$f_{Ca} = \left(\frac{Ca}{Na}\right)_{river} \bigg/ \left(\frac{Ca}{Na}\right)_0 \tag{10}$$

582 Previous research suggested that Ca/Na (molar) values of sediment of the

583 Jinsha mainstream change slightly from Benzilan (3.46) to Panzhihua (2.85)

584 with an average value of 3.20 (Wu et al., 2011). Assuming the $(Ca/Na)_0$ of

585 Jinsha mainstream equals 3.20, then f_{Ca} has a range from 0.16 to 0.34. Similarly,

586 $(Ca/Na)_0$ of Tongtianhe (JS-1) equals 5.6 and its f_{Ca} equals 0.07. Additionally,

587 f_{Ca} values of the Jinsha mainstream show significant correlation with CSI (R^2 =

588 0.82) and pH values (R^2 = 0.93), implying the amount of carbonate precipitation

589 in the Jinsha mainstream ranges from 66% to 93% with an average of 75%.

590   Fig. 9a shows a relationship between measured riverine $\delta^{44/40}$Ca values

591 and Ca/Na ratios of river samples. Both Rayleigh distillation model and

592 equilibrium fractionation processes are examined in the Jinsha mainstream

593 samples, and corresponding fractionation factor values are calculated.

594 According to the equilibrium fractionation model, the Ca isotope composition

595 can be modelled as:

$$\delta^{44/40}Ca_{river} = \delta^{44/40}Ca_0 - 1000(\alpha-1) \times (1-f_{Ca}) \qquad (11)$$

In addition, to evaluate fractionation factors of the Rayleigh distillation model, a standard approach is conducted as follows (Dellinger et al., 2015; Hindshaw et al., 2013; Pogge von Strandmann et al., 2017; Pogge von Strandmann et al., 2012; Zhao et al., 2019):

$$\delta^{44/40}Ca_{river} = \delta^{44/40}Ca_0 + 1000(\alpha-1) \times \ln(f_{Ca}) \qquad (12)$$

where $\delta^{44/40}Ca_{river}$ corresponds to the Ca isotope composition of river water, and mainstream and tributaries of the Jinsha River have similar initial isotopic compositions($\delta^{44/40}Ca_0$=0.64‰).

Different fractionation models lead to variable fractionation factors (α). For the Jinsha mainstream, the range of Ca isotope Rayleigh fractionation factor is 0.99961-0.99983, with a median of 0.99976, which is consistent with basaltic river data that follow a Rayleigh relationship in Iceland (0.9998) (Hindshaw et al., 2013). Whereas, equilibrium fractionation results in a range of 0.99935-0.99963, with a best fit fractionation factor value of 0.99953, which is a little bit higher than the fractionation factor into inorganic calcite (α = 0.9990-0.9995) (Gussone et al., 2005); the difference may come from diverse precipitation rate, difference temperature and solution chemistry.

Selecting 0.99953 as the α value of the equilibrium fractionation, f_{Ca} values of the Jinsha tributaries range from 0.47 to 0.90 based on Eq. (11), which corresponds to the amount of Ca precipitation, which ranges from 10% to 53%, with an average value of 35%. Similarly, choosing 0.99973 as the α value of the

28

Rayleigh fractionation model, according to equation (12), the range of f_{Ca} of the Jinsha tributaries is 0.12-0.66, and the corresponding precipitation range is 34%-88%, with an average of 72%. Moreover, using the batch fractionation model and the optimal fractionation factor, the f_{Ca} of the main stream of the Jinsha River is 0.49-0.66, which is closer to the f_{Ca} calculated based on the sediment composition of the riverbed. However, using the Rayleigh fractionation model and its best fit α value could obtain the f_{Ca} of the Jinsha River mainstream with a range of 0.02-0.13, which overestimates the Ca precipitation amount in the main stream of the Jinsha River. In addition, Rayleigh fractionation requires a closed system, while the river is an open system, so the equilibrium fractionation model is more appropriate. Therefore, the amount of carbonate precipitation in the tributary has a dissolved Ca uptake range of 10%-53%. Considering the range of fractionation factor is from 0.99935 to 0.99963, the uncertainty of the evaluation of the amount of carbonate precipitation is ~10%.

From the above, we suggest that carbonate precipitation has taken place in the Jinsha River, which is congruous with the results obtained by Zhao et al. (2019) through the study of Mg isotopes in the same river.

5.3 Effect of evaporite weathering on Ca isotopes

In Section 5.2.2, f_{Ca} values of the Jinsha River mainstream are lower than those of the tributaries, which may indicate more carbonate has precipitated in

the mainstream. One of the reasons is that weathering of Ca-bearing evaporites,

mainly gypsum, which are widely distributed in the source area of the Jinsha

River, releases more Ca^{2+} into the river water, resulting in a higher saturation

index of carbonate (above zero), which gives rise to precipitation of carbonate

and elevated Ca isotopic compositions of the mainstream river water, since

secondary carbonates incorporate lighter Ca isotopes preferentially (Gussone

et al., 2003; Gussone et al., 2011; Lemarchand et al., 2004; Tang et al., 2008;

Tang et al., 2012; Tipper et al., 2006).

In this study, we evaluated the amount of calcium carbonate precipitation,

and then assessed the effect of evaporite dissolution on calcium carbonate

precipitation and river Ca isotopes. The f_{Ca} values of the tributaries are variable,

ranging from 0.47 to 0.90 with an uncertainty of ~0.1, which indicates that the

proportion of precipitated Ca ranges from 0% to 63% with the average of 35%.

However, f_{Ca} in the mainstream ranges from 0.07 to 0.34 with an average of

0.25, which suggests at least 66% of dissolved Ca has precipitated. This result

is lower than that of the tributaries, but in good agreement with previous studies

which indicated up to 70% of Ca in Himalayan rivers was removed through

carbonate precipitation (Bickle et al., 2005; Jacobson et al., 2002).

Widespread limestone in the Jinsha River Basin releases plenty of

dissolved Ca into the river, and, combined with an arid climate, provides the

necessary conditions for the precipitation of carbonate. Weathering of evaporite

releases more dissolved Ca into river water and increases the precipitation of

carbonate by ~30%. Note that plants growth and clay mineral adsorption and/or incorporation also uptake more Ca than Na, which will reduce riverine Ca/Na ratios and f_{Ca} values. Therefore, what we have obtained is the upper limit of the amount of precipitation.

Further, the influence of evaporite weathering still needs to be evaluated. Ca isotope ratios at the source of the Changjiang river, published by Tipper et al. (2010), are 1.04‰ in summer and by Zhu and MacDougall (1988) as 1.25‰, which is consistent with our results (1.11‰, JS-1). However, Ca isotope ratios at the river mouth have an average of 0.77‰, which is similar to the average value (0.80‰) of the tributaries of the Jinsha River. This suggests that evaporite weathering in the upper reaches of the Changjiang river do not affect its Ca isotopic composition entering into the ocean. Therefore, evaporite weathering could fractionate Ca isotope significantly, but this signal appears to be overprinted by other processes further downstream. In most cases, the influence of evaporite dissolution is limited and only could affect the $\delta^{44/40}Ca$ of small and regional rivers. However, some large rivers may also be affected by evaporite weathering and have higher $\delta^{44/40}Ca$ values than others, such as the Yellow River, which has high Ca isotope ratios in both summer and winter at its estuary (Tipper et al., 2010). Additionally, while investigating the evolution of paleoclimate using stable Ca isotopes, it may necessary to consider the effect of evaporites weathering. For example, when the paleo-temperature is high, the enhanced evaporation leads to the extensive distribution of evaporites, which

684 elevates $\delta^{44/40}$Ca value of the continental weathering flux, and then affect the

685 global Ca mass balance.

686

687 **Conclusion**

688   This study investigated chemical weathering and solute sources

689 constrained by calcium and strontium isotopes in the upper reaches of the

690 Changjiang River. Hydrochemistry of the mainstream is different from that of

691 tributaries, and the contribution order of solute sources is evaporites>

692 carbonates > silicates for the mainstream, while carbonates > silicates >

693 evaporites for tributaries.

694   The $\delta^{44/40}$Ca of the dissolved load in the upper reaches of the Jinsha River

695 ranges from 0.68‰ to 1.11‰ with an average of 0.87‰. The effects of

696 atmospheric input and biological input on the Ca isotope ratio of rivers are minor.

697 The conventional mixing of different rock sources cannot fully explain the Ca

698 isotope ratio of the Jinsha River and secondary processes must be invoked.

699 Owing to a weak negative correlation between the Ca isotope ratios and the

700 saturation indices of silicate clay minerals, adsorption or incorporation is not the

701 main factor that raises the Ca isotope ratio of the river. Combined with the

702 positive correlation between calcite saturation indices and $\delta^{44/40}$Ca values, we

703 believe that calcium carbonate precipitation is the cause of elevated Ca isotope

704 ratios. Moreover, the Equilibrium fractionation model can be used to explaining

705 Ca isotopic compositions of the Jinsha River, and the calculated fractionation

factors are between 0.99935 and 0.99965, which are similar to fractionation known to be caused by calcite precipitation.

Evaporite (mainly gypsum) weathering controls the amount of carbonate precipitation indirectly through the release of Ca^{2+} into the river water which elevates the CSI value. In the dry and cold plateau climate, at least 66% Ca was removed from the mainstream of the Jinsha River while the average value is ~35% in the tributaries, resulting in a heavier Ca isotope ratio in the main stream than in the tributaries. However, the impact of evaporite weathering on carbon budgets of rivers still needs more related research to test.

728 constructive suggestions from the editor and the anonymous reviewers.

729

730 **Reference**

731 Amini, M. et al., 2008. Calcium isotope ($\delta^{44}/^{40}Ca$) fractionation along hydrothermal pathways,
732   Logatchev field (Mid-Atlantic Ridge, 14°45′N). Geochimica et Cosmochimica Acta, 72(16):
733   4107-4122, doi:10.1016/j.gca.2008.05.055.

734 Belshaw, N., Zhu, X., Guo, Y., O'Nions, R., 2000. High precision measurement of iron isotopes by
735   plasma source mass spectrometry. International Journal of Mass Spectrometry, 197(1-3):
736   191-195, doi:10.1016/S1387-3806(99)00245-6.

737 Berner, E.K., Berner, R.A., 2012. Global environment: water, air, and geochemical cycles.

738 Berner, R.A., 2003. The long-term carbon cycle, fossil fuels and atmospheric composition. Nature,
739   426: 323-326, doi:10.1038/nature02131.

740 Berner, R.A., Lasaga, A.C., Garrels, R.M., 1983. The carbonate-silicate geochemical cycle and its
741   effect on atmospheric carbon-dioxide over the past 100 million years. American Journal
742   of Science, 283: 641-683, doi:10.2475/ajs.283.7.641.

743 Bickle, M.J. et al., 2005. Relative contributions of silicate and carbonate rocks to riverine Sr fluxes
744   in the headwaters of the Ganges. Geochimica et Cosmochimica Acta, 69(9): 2221-2240,
745   doi:10.1016/j.gca.2004.11.019.

746 Blättler, C.L., Higgins, J.A., 2014. Calcium isotopes in evaporites record variations in Phanerozoic
747   seawater SO_4 and Ca. Geology, 42(8): 711-714, doi:10.1130/g35721.1.

748 Blättler, C.L., Miller, N.R., Higgins, J.A., 2015. Mg and Ca isotope signatures of authigenic dolomite
749   in siliceous deep-sea sediments. Earth and Planetary Science Letters, 419: 32-42,
750   doi:10.1016/j.epsl.2015.03.006.

751 Böhm, F. et al., 2012. Strontium isotope fractionation of planktic foraminifera and inorganic calcite.
752   Geochimica et Cosmochimica Acta, 93: 300-314, doi:10.1016/j.gca.2012.04.038.

753 Brazier, J.-M. et al., 2019. Calcium isotopic fractionation during adsorption onto and desorption
754   from soil phyllosilicates (kaolinite, montmorillonite and muscovite). Geochimica et
755   Cosmochimica Acta, 250: 324-347, doi:10.1016/j.gca.2019.02.017.

756 Cenki-Tok, B. et al., 2009. The impact of water–rock interaction and vegetation on calcium isotope
757   fractionation in soil- and stream waters of a small, forested catchment (the Strengbach
758   case). Geochimica et Cosmochimica Acta, 73(8): 2215-2228,
759   doi:10.1016/j.gca.2009.01.023.

760 Chetelat, B. et al., 2008. Geochemistry of the dissolved load of the Changjiang Basin rivers:
761   Anthropogenic impacts and chemical weathering. Geochimica et Cosmochimica Acta,
762   72(17): 4254-4277, doi:10.1016/j.gca.2008.06.013.

763 Chu, N.-C., Henderson, G.M., Belshaw, N.S., Hedges, R.E.M., 2006. Establishing the potential of Ca
764   isotopes as proxy for consumption of dairy products. Applied Geochemistry, 21(10): 1656-
765   1667, doi:10.1016/j.apgeochem.2006.07.003.

766 Cobert, F. et al., 2011. Experimental identification of Ca isotopic fractionations in higher plants.
767   Geochimica et Cosmochimica Acta, 75(19): 5467-5482, doi:10.1016/j.gca.2011.06.032.

768 Dellinger, M. et al., 2015. Riverine Li isotope fractionation in the Amazon River basin controlled by

769   the weathering regimes. Geochimica et Cosmochimica Acta, 164: 71-93,
770   doi:10.1016/j.gca.2015.04.042.

771 DePaolo, D.J., 2004. Calcium Isotopic Variations Produced by Biological, Kinetic, Radiogenic and
772   Nucleosynthetic Processes. Reviews in Mineralogy and Geochemistry, 55: 255-288,
773   doi:10.2138/gsrmg.55.1.255.

774 Ding, T. et al., 2013. The contents and mineral and chemical compositions of suspended particulate
775   materials in the Yangtze River, and their geological and environmental implacations. Acta
776   Geologica Sinica, 87(5): 634-660 (*In Chinese with English abstract*).

777 Ewing, S.A. et al., 2008. Non-biological fractionation of stable Ca isotopes in soils of the Atacama
778   Desert, Chile. Geochimica et Cosmochimica Acta, 72(4): 1096-1110,
779   doi:10.1016/j.gca.2007.10.029.

780 Fan, B. et al., 2016. The geochemical behavior of Mg isotopes in the Huanghe basin, China.
781   Chemical Geology, 426: 19-27, doi:10.1016/j.chemgeo.2016.01.005.

782 Fantle, M.S., 2010. Evaluating the Ca isotope proxy. American Journal of Science, 310(3): 194-230,
783   doi:10.2475/03.2010.03.

784 Fantle, M.S., 2015. Calcium isotopic evidence for rapid recrystallization of bulk marine carbonates
785   and implications for geochemical proxies. Geochimica et Cosmochimica Acta, 148: 378-
786   401, doi:10.1016/j.gca.2014.10.005.

787 Fantle, M.S., DePaolo, D.J., 2005. Variations in the marine Ca cycle over the past 20 million years.
788   Earth and Planetary Science Letters, 237(1-2): 102-117, doi:10.1016/j.epsl.2005.06.024.

789 Fantle, M.S., Tipper, E.T., 2014. Calcium isotopes in the global biogeochemical Ca cycle:
790   Implications for development of a Ca isotope proxy. Earth-Science Reviews, 129: 148-177,
791   doi:10.1016/j.earscirev.2013.10.004.

792 Farkaš, J. et al., 2007. Calcium isotope record of Phanerozoic oceans: Implications for chemical
793   evolution of seawater and its causative mechanisms. Geochimica et Cosmochimica Acta,
794   71(21): 5117-5134, doi:10.1016/j.gca.2007.09.004.

795 Farkaš, J., Déjeant, A., Novák, M., Jacobsen, S.B., 2011. Calcium isotope constraints on the uptake
796   and sources of Ca^{2+} in a base-poor forest: A new concept of combining stable ($\delta^{44/42}Ca$)
797   and radiogenic (εCa) signals. Geochimica et Cosmochimica Acta, 75(22): 7031-7046,
798   doi:10.1016/j.gca.2011.09.021.

799 Gaillardet, J., Allegre, C.J., Dupre, B., Louvat, P., 1999. Global silicate weathering and CO_2
800   consumption rates deduced from the chemistry of large rivers. Chemical Geology, 159: 3-
801   30, doi:10.1016/S0009-2541(99)00031-5.

802 Gaillardet, J., Calmels, D., Romero-Mujalli, G., Zakharova, E., Hartmann, J., 2018. Global climate
803   control on carbonate weathering intensity. Chemical Geology,
804   doi:10.1016/j.chemgeo.2018.05.009.

805 Galy, A., France-Lanord, C., 1999. Weathering processes in the Ganges–Brahmaputra basin and
806   the riverine alkalinity budget. Chemical Geology, 159: 31-60, doi:10.1016/S0009-
807   2541(99)00033-9.

808 Gislason, S.R., Arnorsson, S., Armannsson, H., 1996. Chemical weathering of basalt in Southwest
809   Iceland; effects of runoff, age of rocks and vegetative/glacial cover. American Journal of
810   Science, 296(8): 837-907, doi:10.2475/ajs.296.8.837.

811 Gussone, N. et al., 2005. Calcium isotope fractionation in calcite and aragonite. Geochimica et
812   Cosmochimica Acta, 69(18): 4485-4494, doi:10.1016/j.gca.2005.06.003.

813 Gussone, N., Dietzel, M., 2016. Calcium Isotope Fractionation During Mineral Precipitation from
814   Aqueous Solution, in : Nikolaus Gussone et al., Calcium Stable Isotope Geochemistry.
815   Advances in Isotope Geochemistry. Springer, Berlin, Heidelberg.

816 Gussone, N. et al., 2003. Model for kinetic effects on calcium isotope fractionation (δ^{44}Ca) in
817   inorganic aragonite and cultured planktonic foraminifera. Geochimica et Cosmochimica
818   Acta, 67(7): 1375-1382, doi:10.1016/s0016-7037(02)01296-6.

819 Gussone, N., Nehrke, G., Teichert, B.M.A., 2011. Calcium isotope fractionation in ikaite and vaterite.
820   Chemical Geology, 285(1-4): 194-202, doi:10.1016/j.chemgeo.2011.04.002.

821 Han, G., Song, Z., Tang, Y., Wu, Q., Wang, Z., 2019. Ca and Sr isotope compositions of rainwater
822   from Guiyang city, Southwest China: Implication for the sources of atmospheric aerosols
823   and their seasonal variations. Atmospheric Environment, 214,
824   doi:10.1016/j.atmosenv.2019.116854.

825 Harouaka, K., Eisenhauer, A., Fantle, M.S., 2014. Experimental investigation of Ca isotopic
826   fractionation during abiotic gypsum precipitation. Geochimica et Cosmochimica Acta, 129:
827   157-176, doi:10.1016/j.gca.2013.12.004.

828 He, M.-Y., Zheng, H.-B., Huang, X.-T., Jia, J.-T., Li, L., 2011. Clay Mineral Assemblages in the
829   Yangtze Drainage and Provenance Implications. Acta Sedimentologica Sinica, 29(3): 544-
830   551 *(in Chinese with English abstract)*. doi:10.14027/j.cnki.cjxb.2011.03.006.

831 Henderson, G.M., Chu, N.C., Bayon, G., Benoit, M., 2006. $\delta^{44/42}$Ca in gas hydrates, porewaters and
832   authigenic carbonates from Niger Delta sediments. Geochimica et Cosmochimica Acta,
833   70(18), doi:10.1016/j.gca.2006.06.493.

834 Hensley, T., 2006. Calcium isotope variation in marine evaporates and carbonates, applications to
835   late Miocene Mediterranean brine chemistry and late Cenozoic calcium cycling in the
836   oceans, UC San Diego.

837 Heuser, A., Schmitt, A.-D., Gussone, N., Wombacher, F., 2016. Analytical Methods. In: Nikolaus
838   Gussone et al., Calcium Stable Isotope Geochemistry. Advances in Isotope Geochemistry.
839   Springer, Berlin,Heidelberg.

840 Hindshaw, R.S., Bourdon, B., Pogge von Strandmann, P.A.E., Vigier, N., Burton, K.W., 2013. The
841   stable calcium isotopic composition of rivers draining basaltic catchments in Iceland. Earth
842   and Planetary Science Letters, 374: 173-184, doi:10.1016/j.epsl.2013.05.038.

843 Hindshaw, R.S. et al., 2012. Calcium isotope fractionation in alpine plants. Biogeochemistry, 112(1-
844   3): 373-388, doi:10.1007/s10533-012-9732-1.

845 Hindshaw, R.S., Reynolds, B.C., Wiederhold, J.G., Kretzschmar, R., Bourdon, B., 2011. Calcium
846   isotopes in a proglacial weathering environment: Damma glacier, Switzerland. Geochimica
847   et Cosmochimica Acta, 75(1): 106-118, doi:10.1016/j.gca.2010.09.038.

848 Holmden, C., 2009. Ca isotope study of Ordovician dolomite, limestone, and anhydrite in the
849   Williston Basin: Implications for subsurface dolomitization and local Ca cycling. Chemical
850   Geology, 268(3-4): 180-188, doi:10.1016/j.chemgeo.2009.08.009.

851 Holmden, C., Bélanger, N., 2010. Ca isotope cycling in a forested ecosystem. Geochimica et
852   Cosmochimica Acta, 74(3): 995-1015, doi:10.1016/j.gca.2009.10.020.

853 Jacobson, A.D., Blum, J.D., Chamberlain, C.P., Poage, M.A., Sloan, V.F., 2002. Ca/Sr and Sr isotope
854   systematics of a Himalayan glacial chronosequence: Carbonate versus silicate weathering
855   rates as a function of landscape surface age. Geochimica et Cosmochimica Acta, 66(1):
856   13-27, doi:10.1016/S0016-7037(01)00755-4.

857 Jacobson, A.D., Grace Andrews, M., Lehn, G.O., Holmden, C., 2015. Silicate versus carbonate
858   weathering in Iceland: New insights from Ca isotopes. Earth and Planetary Science Letters,
859   416: 132-142, doi:10.1016/j.epsl.2015.01.030.

860 Jacobson, A.D., Holmden, C., 2008. δ^{44}Ca evolution in a carbonate aquifer and its bearing on the
861   equilibrium isotope fractionation factor for calcite. Earth and Planetary Science Letters,
862   270(3-4): 349-353, doi:10.1016/j.epsl.2008.03.039.

863 Jacobson, A.D., Wasserburg, G.J., 2005. Anhydrite and the Sr isotope evolution of groundwater in
864   a   carbonate   aquifer.   Chemical   Geology,   214(3-4):   331-350,
865   doi:10.1016/j.chemgeo.2004.10.006.

866 Lehn, G.O. et al., 2017. Constraining seasonal active layer dynamics and chemical weathering
867   reactions occurring in North Slope Alaskan watersheds with major ion and isotope ($\delta^{34}S_{SO4}$,
868    $\delta^{13}C_{DIC}$, $^{87}Sr/^{86}Sr$, $\delta^{44/40}Ca$, and $\delta^{44/42}Ca$) measurements. Geochimica et Cosmochimica Acta,
869   217: 399-420, doi:10.1016/j.gca.2017.07.042.

870 Lemarchand, D., Wasserburg, G.J., Papanastassiou, D.A., 2004. Rate-controlled calcium isotope
871   fractionation in synthetic calcite. Geochimica et Cosmochimica Acta, 68(22): 4665-4678,
872   doi:10.1016/j.gca.2004.05.029.

873 Liu, X.-W., 2016. Preliminary study on characteristics of Meteorological factors and runoff Law in
874   Jinsha River Basin *(in Chinese with English abstract)*.

875 Lu, L., Wang, Q., Wang, G.-Q., Liu, Y.-L., Liu, C.-S., 2016. Trend of Climate Change over the Recent
876   60 Years and its Hydrological Responses for Jinsha River Basin. Journal of Noah China
877   University of Water Resources and Electric Power (Natural Science Edition), 37(5): 16-21
878   *(in Chinese with English abstract)*.

879 Ludwik Halicz, A.G., Nick S. Belshaw and R. Keith O'Nions, 1999. High-precision measurement of
880   calcium isotopes in carbonates and related materials by multiple collector inductively
881   coupled plasma mass spectrometry (MC-ICP-MS). Journal of Analytical Atomic
882   Spectrometry, 14: 1835-1838.

883 Marie-Laure Bagard et al., 2013. Biogeochemistry of stable Ca and radiogenic Sr isotopes in a
884   larch-covered permafrost-dominated watershed of Central Siberia. Geochimica et
885   Cosmochimica Acta, 114: 169-187, doi:10.1016/j.gca.2013.03.038.

886 Marie-Laure Bagard et al., 2011. Seasonal variability of element fluxes in two Central Siberian rivers
887   draining high latitude permafrost dominated areas. Geochimica et Cosmochimica Acta,
888   75(12): 3335-3357, doi:10.1016/j.gca.2011.03.024.

889 Moore, J., Jacobson, A.D., Holmden, C., Craw, D., 2013. Tracking the relationship between
890   mountain uplift, silicate weathering, and long-term CO_2 consumption with Ca isotopes:
891   Southern   Alps,   New   Zealand.   Chemical   Geology,   341:   110-127,
892   doi:10.1016/j.chemgeo.2013.01.005.

893 Nan, X. et al., 2015. High-precision barium isotope measurements by MC-ICP-MS. Journal of
894   Analytical Atomic Spectrometry, 30(11): 2307-2315, doi:10.1039/c5ja00166h.

895 Nielsen, L.C., DePaolo, D.J., 2013. Ca isotope fractionation in a high-alkalinity lake system: Mono
896   Lake,   California.   Geochimica   et   Cosmochimica   Acta,   118:   276-294,
897   doi:10.1016/j.gca.2013.05.007.

898 Noh, H., Huh, Y., Qin, J., Ellis, A., 2009. Chemical weathering in the Three Rivers region of Eastern
899   Tibet.   Geochimica   et   Cosmochimica   Acta,   73(7):   1857-1877,
900   doi:10.1016/j.gca.2009.01.005.

901 Ockert, C., Gussone, N., Kaufhold, S., Teichert, B.M.A., 2013. Isotope fractionation during Ca
902   exchange on clay minerals in a marine environment. Geochimica et Cosmochimica Acta,
903   112: 374-388, doi:10.1016/j.gca.2012.09.041.
904 Oehlerich, M. et al., 2015. Lateglacial and Holocene climatic changes in south-eastern Patagonia
905   inferred from carbonate isotope records of Laguna Potrok Aike (Argentina). Quaternary
906   Science Reviews, 114: 189-202, doi:10.1016/j.quascirev.2015.02.006.
907 Oelkers, E.H., Pogge von Strandmann, P.A.E., Mavromatis, V., 2019. The rapid resetting of the Ca
908   isotopic signatures of calcite at ambient temperature during its congruent dissolution,
909   precipitation, and at equilibrium. Chemical Geology, 512: 1-10,
910   doi:10.1016/j.chemgeo.2019.02.035.
911 Owen, R.A. et al., 2016. Calcium isotopes in caves as a proxy for aridity: Modern calibration and
912   application to the 8.2 kyr event. Earth and Planetary Science Letters, 443: 129-138,
913   doi:10.1016/j.epsl.2016.03.027.
914 Parkhurst, D.L., Appelo, C.A.J., 1999. User's guide to PHREEQC (Version 2): A computer program
915   for speciation, batch-reaction, one-dimensional transport, and inverse geochemical
916   calculations. Water-Resources Investigations Report.
917 Pearce, C.R., Saldi, G.D., Schott, J., Oelkers, E.H., 2012. Isotopic fractionation during congruent
918   dissolution, precipitation and at equilibrium: Evidence from Mg isotopes. Geochimica et
919   Cosmochimica Acta, 92: 170-183, doi:10.1016/j.gca.2012.05.045.
920 Pogge von Strandmann, P.A.E. et al., 2019a. Rapid CO_2 mineralisation into calcite at the CarbFix
921   storage site quantified using calcium isotopes. Nature Communication, 10(1): 1983,
922   doi:10.1038/s41467-019-10003-8.
923 Pogge von Strandmann, P.A.E., Frings, P.J., Murphy, M.J., 2017. Lithium isotope behaviour during
924   weathering in the Ganges Alluvial Plain. Geochimica et Cosmochimica Acta, 198: 17-31,
925   doi:10.1016/j.gca.2016.11.017.
926 Pogge von Strandmann, P.A.E., Hendry, K.R., Hatton, J.E., Robinson, L.F., 2019b. The Response of
927   Magnesium, Silicon, and Calcium Isotopes to Rapidly Uplifting and Weathering Terrains:
928   South Island, New Zealand. Frontiers in Earth Science, 7, doi:10.3389/feart.2019.00240.
929 Pogge von Strandmann, P.A.E., Jenkyns, H.C., Woodfine, R.G., 2013. Lithium isotope evidence for
930   enhanced weathering during Oceanic Anoxic Event 2. Nature Geoscience, 6(8): 668-672,
931   doi:10.1038/ngeo1875.
932 Pogge von Strandmann, P.A.E., Olsson, J., Luu, T.-H., Gislason, S.R., Burton, K.W., 2019c. Using Mg
933   Isotopes to Estimate Natural Calcite Compositions and Precipitation Rates During the
934   2010 Eyjafjallajökull Eruption. Frontiers in Earth Science, 7, doi:10.3389/feart.2019.00006.
935 Pogge von Strandmann, P.A.E. et al., 2012. Lithium, magnesium and silicon isotope behaviour
936   accompanying weathering in a basaltic soil and pore water profile in Iceland. Earth and
937   Planetary Science Letters, 339-340: 11-23, doi:10.1016/j.epsl.2012.05.035.
938 Rocha, C.L.D.L., DePaolo, D.J., 2000. Isotopic evidence for variations in the marine calcium cycle
939   over the Cenozoic. Science, 289(5482): 1176-1178, doi:10.1126/science.289.5482.1176.
940 Rudnick, R.L., Gao, S., 2014. Composition of the Continental Crust, in : Karl Turekian and Heinrich
941   Holland, Treatise on Geochemistry., pp. 1-51.
942 Russell, W.A., Papanastassiou, D.A., Tombrello, T.A., 1978. Ca isotope fractionation on the Earth
943   and other solar system materials. 42: 1075-1090, doi:0016-7037/78/0801-1075$02.00/0.
944 Ryu, J.-S., Jacobson, A.D., Holmden, C., Lundstrom, C., Zhang, Z., 2011. The major ion, $\delta^{44/40}$Ca,

945        $\delta^{44/42}$Ca, and $\delta^{26/24}$Mg geochemistry of granite weathering at pH=1 and T=25°C: power-
946   law processes and the relative reactivity of minerals. Geochimica et Cosmochimica Acta,
947   75(20): 6004-6026, doi:10.1016/j.gca.2011.07.025.

948 Schmitt, A.-D., 2016. Earth-Surface Ca Isotopic Fractionations, in : Nikolaus Gussone et al, Calcium
949   Stable Isotope Geochemistry. Advances in Isotope Geochemistry. Springer, Berlin,
950   Heidelberg, pp. 145-172.

951 Schmitt, A.-D., Chabaux, F., Stille, P., 2003. The calcium riverine and hydrothermal isotopic fluxes
952   and the oceanic calcium mass balance. Earth and Planetary Science Letters, 213(3-4): 503-
953   518, doi:10.1016/s0012-821x(03)00341-8.

954 Schmitt, A.-D., Gangloff, S., Labolle, F., Chabaux, F., Stille, P., 2017. Calcium biogeochemical cycle
955   at the beech tree-soil solution interface from the Strengbach CZO (NE France): insights
956   from stable Ca and radiogenic Sr isotopes. Geochimica et Cosmochimica Acta, 213: 91-
957   109, doi:10.1016/j.gca.2017.06.039.

958 Stefánsson, A., Gíslason, S.R., 2001. Chemical Weathering of Basalts, Southwest Iceland: Effect of
959   Rock Crystallinity and Secondary Minerals on Chemical Fluxes to the Ocean. American
960   Journal of Science, 301(6): 513-556, doi:10.2475/ajs.301.6.513.

961 Steuber, T., Buhl, D., 2006. Calcium-isotope fractionation in selected modern and ancient marine
962   carbonates. Geochimica et Cosmochimica Acta, 70(22): 5507-5521,
963   doi:10.1016/j.gca.2006.08.028.

964 Su, Z.-H., Chen, W.-Z., 2016. Runoff in Source Region of the Yangtze River in Recent 60 Years:
965   Variation Characteristics and Trend Analysis. Chinese Agricultural Science Bulletin, 32(34):
966   166-171 *(in Chinese with English abstract)*.

967 Sun, J. et al., 2019. A one-column separation of Ca and Sr for isotopic analysis using MC-ICPMS
968   Goldschmidt.

969 Tang, J., Dietzel, M., Böhm, F., Köhler, S.J., Eisenhauer, A., 2008. Sr^{2+}/Ca^{2+} and $^{44}Ca/^{40}Ca$ fractionation
970   during inorganic calcite formation: II. Ca isotopes. Geochimica et Cosmochimica Acta,
971   72(15): 3733-3745, doi:10.1016/j.gca.2008.05.033.

972 Tang, J. et al., 2012. Sr^{2+}/Ca^{2+} and $^{44}Ca/^{40}Ca$ fractionation during inorganic calcite formation: III.
973   Impact of salinity/ionic strength. Geochim Cosmochim Acta, 77(C): 432-443,
974   doi:10.1016/j.gca.2011.10.039.

975 Teichert, B.M.A., Gussone, N., Eisenhauer, A., Bohrmann, G., 2005. Clathrites: Archives of near-
976   seafloor pore-fluid evolution ($\delta^{44/40}$Ca, δ^{13}C, δ^{18}O) in gas hydrate environments. Geology,
977   33(3): 213-216, doi:10.1130/g21317.1.

978 Tipper, E., Galy, A., Bickle, M., 2006. Riverine evidence for a fractionated reservoir of Ca and Mg on
979   the continents: Implications for the oceanic Ca cycle. Earth and Planetary Science Letters,
980   247(3-4): 267-279, doi:10.1016/j.epsl.2006.04.033.

981 Tipper, E.T. et al., 2010. Calcium isotope ratios in the world's largest rivers: A constraint on the
982   maximum imbalance of oceanic calcium fluxes. Global Biogeochemical Cycles, 24(3),
983   doi:10.1029/2009gb003574.

984 Tipper, E.T., Galy, A., Bickle, M.J., 2008. Calcium and magnesium isotope systematics in rivers
985   draining the Himalaya-Tibetan-Plateau region: Lithological or fractionation control?
986   Geochimica et Cosmochimica Acta, 72(4): 1057-1075, doi:10.1016/j.gca.2007.11.029.

987 Tipper, E.T., Schmitt, A.-D., Gussone, N., 2016. Global Ca Cycles: Coupling of Continental and
988   Oceanic Processes, in Nikolaus Gussone et al., Calcium Stable Isotope Geochemistry.

989   Advances in Isotope Geochemistry, pp. 173-222.

990   Torres, M.A., West, A.J., Clark, K.E., 2015. Geomorphic regime modulates hydrologic control of
991   chemical weathering in the Andes–Amazon. Geochimica et Cosmochimica Acta, 166: 105-
992   128, doi:10.1016/j.gca.2015.06.007.

993   Walker, J.C.G., Hays, P.B., Kasting, J.F., 1981. A negative feedback mechanism for the long-term
994   stabilization of Earth's surface temperature. Journal of Geophysical Research, 86(C10):
995   9776-9782, doi:10.1029/JC086iC10p09776.

996   Wang, S. et al., 2012. Calcium isotope fractionation and its controlling factors over authigenic
997   carbonates in the cold seeps of the northern South China Sea. Chinese Science Bulletin,
998   57(11): 1325-1332, doi:10.1007/s11434-012-4990-9.

999   Wang, S. et al., 2013. Factors influencing methane-derived authigenic carbonate formation at cold
1000   seep from southwestern Dongsha area in the northern South China Sea. Environmental
1001   Earth Sciences, 71(5): 2087-2094, doi:10.1007/s12665-013-2611-9.

1002   Wang, Y.-s., Chen, X.-x., Zhang, M.-n., 2018. Hydrochemistry and Chemical Weathering Processes
1003   of Malian River Basin. Earth and Environment, 46(1): 15-22 (*in Chinese with English
1004   abstract*).

1005   Wellman, H., Wilson, A., 1965. Salt Weathering, a Neglected Geological Erosive Agent in Coastal
1006   and Arid Environments. Nature, 205(1097-1098), doi:10.1038/2051097a0.

1007   West, A., Galy, A., Bickle, M., 2005. Tectonic and climatic controls on silicate weathering. Earth and
1008   Planetary Science Letters, 235(1-2): 211-228, doi:10.1016/j.epsl.2005.03.020.

1009   White, A.F., Blum, A.E., 1995. Effects of climate on chemical_ weathering in watersheds. Geochimica
1010   et Cosmochimica Acta, 59(9): 1729-1747, doi:10.1016/0016-7037(95)00078-E.

1011   Wiegand, B.A., Schwendenmann, L., 2013. Determination of Sr and Ca sources in small tropical
1012   catchments (La Selva, Costa Rica) – A comparison of Sr and Ca isotopes. Journal of
1013   Hydrology, 488: 110-117, doi:10.1016/j.jhydrol.2013.02.044.

1014   Wu, W. et al., 2011. Mineralogy, major and trace element geochemistry of riverbed sediments in
1015   the headwaters of the Yangtze, Tongtian River and Jinsha River. Journal of Asian Earth
1016   Sciences, 40(2): 611-621, doi:10.1016/j.jseaes.2010.10.013.

1017   Wu, W., Xu, S., Yang, J., Yin, H., Tao, X., 2009a. Sr fluxes and isotopic compositions in the
1018   headwaters of the Yangtze River, Tongtian River and Jinsha River originating from the
1019   Qinghai–Tibet Plateau. Chemical Geology, 260(1-2): 63-72,
1020   doi:10.1016/j.chemgeo.2008.12.007.

1021   Wu, W. et al., 2009b. Sr fluxes and isotopic compositions of the eleven rivers originating from the
1022   Qinghai-Tibet Plateau and their contributions to [87]Sr/[86]Sr evolution of seawater. Science in
1023   China Series D: Earth Sciences, 52(8): 1059-1067, doi:10.1007/s11430-009-0084-1.

1024   Wu, W., Yang, J., Xu, S., Yin, H., 2008. Geochemistry of the headwaters of the Yangtze River,
1025   Tongtian He and Jinsha Jiang: Silicate weathering and CO_2 consumption. Applied
1026   Geochemistry, 23(12): 3712-3727, doi:10.1016/j.apgeochem.2008.09.005.

1027   Wu, W., Zheng, H., Xu, S., Yang, J., Liu, W., 2013. Trace element geochemistry of riverbed and
1028   suspended sediments in the upper Yangtze River. Journal of Geochemical Exploration,
1029   124: 67-78, doi:10.1016/j.gexplo.2012.08.005.

1030   Xie, X., Li, H., Ju, Y., Chang, G., 2018. Analysis of Hydrological characteristics in Jinsha River Basin.
1031   Sichuan Water Resources, 6: 101-104 (*in Chinese with English abstract*).

1032   Yu, S., Tang, Y., 1980. Hydrochemical characteristics of the saline lakes on the Qinghai-Xizang

1033   plateau, Proceedings of Symposium on Qinghai-Xizang (Tibet) Plateau, , Beijing, China.,
1034   pp. 248.
1035   Zhang, L.-L. et al., 2016. Characteristics of water chemistry and its indication of chemical
1036   weathering in Jinshajiang, Lancangjiang and Nujiang drainage basins. Environmental Earth
1037   Sciences, 75(6), doi:10.1007/s12665-015-5115-y.
1038   Zhang, N., He, Y., Cao, J., Ho, K., Shen, Z., 2012. Long-term trends in chemical composition of
1039   precipitation at Lijiang, southeast Tibetan Plateau, southwestern China. Atmospheric
1040   Research, 106: 50-60, doi:10.1016/j.atmosres.2011.11.006.
1041   Zhang, X.-F., Yan, H.-c., Yao, Y., Lu, Y.-T., 2018. Analysis on the Sectional Annual Runoff Change
1042   of the Jinsha River Basin in the Recent 50 Years. Resources and Environment in the Yangtze
1043   Basin, 27(10): 2283-2292 *(in Chinese with English abstract)*.
1044   Zhao, J.-C. et al., 2003. Origin of major elements and Sr isotope for river water in Yangtze River
1045   source area. Hydrogeology & Engineering Geology(2): 89-93 *(in Chinese with English*
1046   *abstract)*.
1047   Zhao, T. et al., 2019. The influence of carbonate precipitation on riverine magnesium isotope
1048   signals: new constrains from Jinsha River Basin, Southeast Tibetan Plateau. Geochimica et
1049   Cosmochimica Acta, 248: 172-184, doi:10.1016/j.gca.2019.01.005.
1050   Zhong, J., 2017. Chemical weathering and carbon biogeochemical processes in the upper
1051   Changjiang Basin impacted by the hydrological conditions, The University of Chinese
1052   Academy of Sciences (*in Chinese with English abstract*).
1053   Zhu, P., Macdougall, J.D., 1988. Calcium isotopes in the marine environment and the oceanic
1054   calcium cycle. Geochim Cosmochim Acta, 62(10): 1691-1698, doi:10.1016/S0016-
1055   7037(98)00110-0.

1056

1057

1058

1059

1060

1061

1062

1063

1064

1065

1066

1067

1068

1069

1070

1071

1072

1073

1074

Table 1. Chemical composition, Ca and Sr isotopic composition of the Jinsha River water.

Labels	Sample ID	T °C	pH	NDVI[a] %	Ca[b] μmol/L	Mg[b] μmol/L	Na[b] μmol/L	K[b] μmol/L	Si[b] μmol/L	Alk[b] μmol/L	SO$_4$[b] μmol/L	Cl[b] μmol/L	NO$_3$[b] μmol/L	Sr μmol/L	δ$^{44/40}$Ca ‰	2sd	^{87}Sr/^{86}Sr	2sd
Mainstream																		
JS-1	Mainstream	15.3	8.66	0.23	1341	878	5555	127	91	2973	1152	5183	30	9.35	1.11	0.14	0.7098	2.81E-05
JS-4	Mainstream	14.3	8.56	0.42	1213	759	4115	97	86	2847	923	3590	26	6.92	0.94	0.14	0.7101	2.73E-05
JS-7	Mainstream	16.8	8.47	0.46	920	463	1853	53	89	2162	520	1792	16	3.93	0.89	0.14	0.7107	2.61E-05
JS-10	Mainstream	17.9	8.46	0.47	861	418	1771	59	87	1273	481	1604	17	3.60	0.99	0.14	0.7106	2.34E-05
JS-12	Mainstream	18.2	8.43	--	803	372	1372	51	90	1772	398	1253	12	2.99	1.02	0.10	0.7108	3.50E-05
JS-15	Mainstream	16.6	8.42	--	770	347	1235	37	92	1064	358	1106	16	2.70	0.87	0.10	0.7108	2.31E-05
JS-20	Mainstream	21.4	8.35	0.53	920	447	1546	36	101	1956	443	1370	22	3.17	1.07	0.14	0.7105	2.80E-05
Tributaries																		
JS-2	Tongtian Rive	16.1	8.48	0.53	1134	580	252	20	72	2442	492	46	28	2.96	0.84	0.14	--	--
JS-3	Se Qu	16.5	8.28	0.51	957	585	165	26	83	2681	266	28	21	1.77	0.88	0.14	0.7142	2.51E-05
JS-5	Zhen Qu	14.8	8.32	0.73	530	219	98	15	95	1287	99	28	10	0.78	0.75	0.10	0.7144	2.72E-05
JS-6	Ba Qu	12.7	8.25	0.42	755	288	112	30	88	2002	339	6	6	1.48	0.78	0.14	0.7157	2.32E-05
JS-8	Zong Qu	16.9	8.17	0.49	600	175	109	24	97	1412	54	12	15	0.76	0.83	0.14	0.7130	2.11E-05
JS-9	Ding Qu	14.4	8.23	0.46	538	158	81	32	93	1902	72	10	5	0.81	0.68	0.14	0.7126	2.31E-05
JS-11	Gang Qu	15.7	8.44	0.61	827	257	96	16	82	1751	172	12	5	2.27	0.75	0.10	0.7090	2.31E-05
JS-13	Zhubaluo Rive	15.1	8.41	0.63	469	72	41	7	71	940	48	7	3	0.64	0.81	0.14	0.7118	2.48E-05
JS-14	Chongjiang Ri	15.5	8.23	0.60	453	117	47	21	107	1695	15	12	14	0.81	0.74	0.14	0.7102	2.75E-05
JS-16	Shuoduogang	12.8	8.14	0.56	712	230	80	10	84	1719	42	9	4	1.11	0.87	0.14	0.7091	2.31E-05
JS-18	Renli River	22.4	8.06	0.56	920	400	195	39	113	2304	101	75	43	1.19	0.83	0.14	0.7108	2.98E-05
Gypsum																		
G1-1	near Dang Qu														0.27	0.10		
G1-2	near Dang Qu														0.24	0.10		
G2	near Tuotuohe														0.80	0.10		
G3-1	near Tuotuohe														0.80	0.10		
G3-2	near Tuotuohe														0.95	0.10		

1075

(a) NDVI: The Normalized Difference Vegetation Index calculated by GIS. (b) Major element data from Zhong (2017).

1076

1077

1078

43

1079

1080 **Table 2.** Saturation Index of carbonates and clay minerals in the Jinsha River.

River labels	Mineral types						
	Calcite	Dolomite	Illite	Chlorite	Montmorillonite	Kalinite	Kmica
Saturation index of minerals (SI)							
Mainstream							
JS-1	0.93	1.67	-0.39	3.60	2.96	1.32	4.98
JS-4	0.79	1.35	-0.29	2.34	2.86	1.60	5.18
JS-7	0.56	0.84	-0.28	1.58	2.69	1.83	5.21
JS-10	0.32	0.36	-0.34	1.59	2.67	1.77	5.19
JS-12	0.42	0.54	-0.04	1.48	2.89	2.09	5.88
JS-15	0.16	-0.01	0.10	1.02	2.89	2.29	5.71
JS-20	0.47	0.72	-0.83	1.40	2.71	1.47	4.47
Tributaries							
JS-2	0.71	1.14	-1.94	0.76	1.49	0.68	3.07
JS-3	0.51	0.82	-0.62	0.24	2.29	1.88	4.80
JS-5	0.01	-0.38	-0.24	-1.27	2.38	2.33	5.24
JS-6	0.22	-0.03	0.93	-1.26	2.94	3.28	6.86
JS-8	-0.01	-0.54	0.20	-2.20	2.70	2.73	5.95
JS-9	0.08	-0.38	1.74	-1.36	3.56	4.00	7.98
JS-11	0.44	0.37	-0.40	0.16	2.35	2.11	5.08
JS-13	0.07	-0.96	-0.73	-2.84	1.80	2.21	4.84
JS-14	-0.01	-0.60	0.60	-2.51	2.88	3.05	6.40
JS-16	0.05	-0.44	0.52	-2.68	2.64	3.30	6.33
JS-18	0.32	0.37	-0.01	-0.31	3.13	2.38	5.60

1081

1082

1083

1084

1085

1086

1087

1088

1089

1090   **Table 3.** The fractionation factor and the amount of Ca precipitation in the

1091   Jinsha River water.

River labels	Equilibrium fractionation model					
	α = 0.99935		α = 0.99953		α = 0.99963	
	f_{Ca}	Removed Ca(%)	f_{Ca}	Removed Ca(%)	f_{Ca}	Removed Ca(%)
Mainstream						
JS-1	0.07	93	0.07	93	0.07	93
JS-4	0.16	84	0.16	84	0.16	84
JS-7	0.27	73	0.27	73	0.27	73
JS-10	0.26	74	0.26	74	0.26	74
JS-12	0.32	68	0.32	68	0.32	68
JS-15	0.34	66	0.34	66	0.34	66
JS-20	0.32	68	0.32	68	0.32	68
Tributaries						
JS-2	0.68	32	0.55	45	0.43	57
JS-3	0.62	38	0.47	53	0.32	68
JS-5	0.82	18	0.75	25	0.69	31
JS-6	0.77	23	0.68	32	0.59	41
JS-8	0.70	30	0.58	42	0.47	53
JS-9	0.92	8	0.90	10	0.87	13
JS-11	0.82	18	0.75	25	0.68	32
JS-13	0.72	28	0.62	38	0.51	49
JS-14	0.83	17	0.76	24	0.70	30
JS-16	0.63	37	0.49	51	0.35	65
JS-18	0.69	31	0.57	43	0.46	54

1092

1093

1094

1095

1096

1097

1098

Figure captions
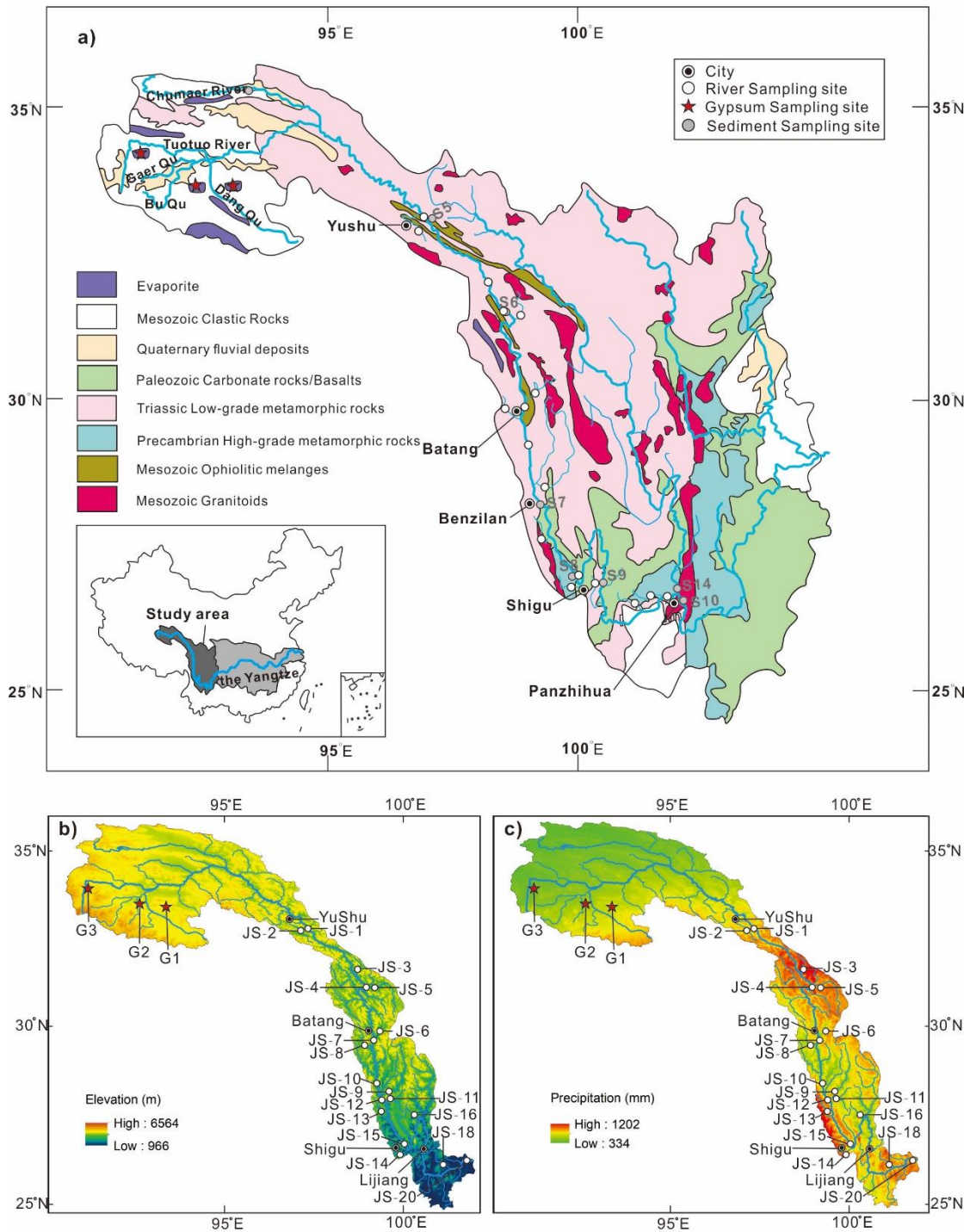
Fig. 1. (a) Geological map of the headwaters of the Changjiang River and the Jinsha River basin, modified from (Wu et al., 2011); (b) and (c) show elevation and precipitation of the Jinsha River basin separately. White solid circles represent the river sampling site of this study, grey solid circles (S5-S14) are

1105 sediment sampling locations in previous research (Wu et al., 2011), red stars

1106 represent gypsum sampling sites and the concentric circles are cities.

1107
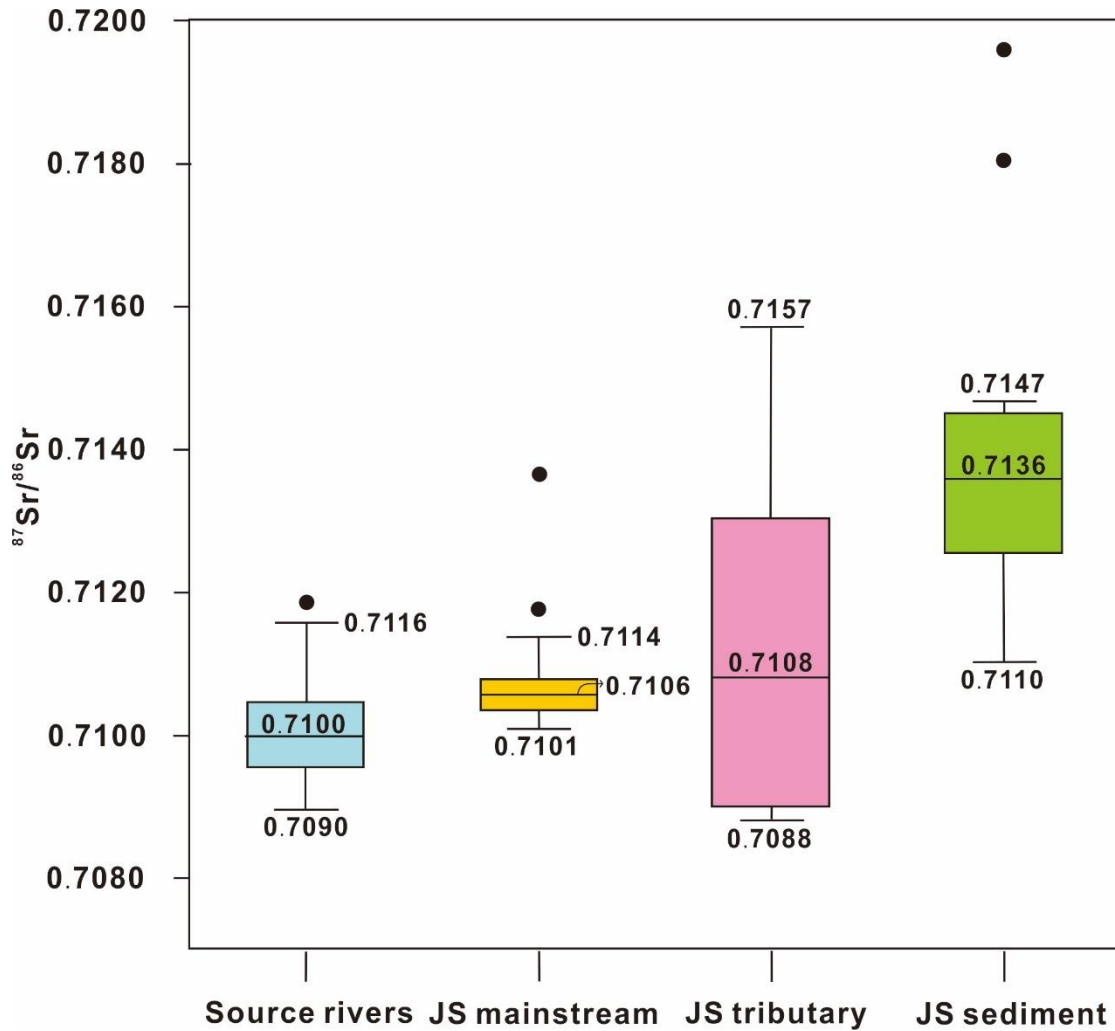
1108

1109 **Fig. 2.** Sr isotopic compositions in the Jinsha River basin. Each box consists

1110 of a rectangle and three horizontal lines. Those horizontal lines represent the

1111 min value, median value and max value of the data separately from bottom to

1112 upper. The bottom horizontal line of the rectangle represents the first quartile

1113 (25%), which is the median of the data points lower than the median. And

1114 median is the second quartile. On the contrary, the top horizontal line

1115 represents the third quartile (75%), which is the median of the data points

higher than the median. The black dots mean abnormal values.
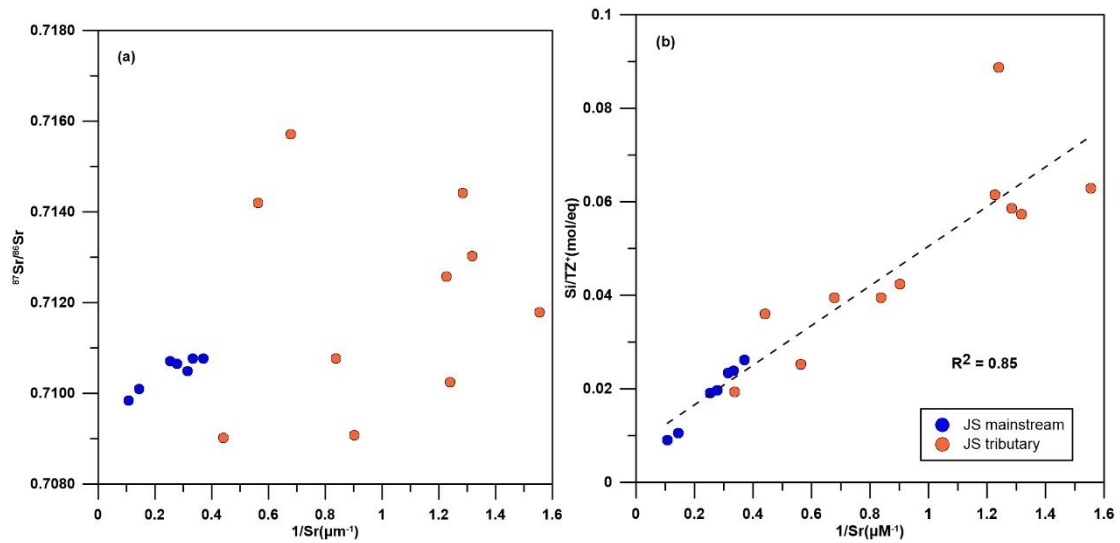
Fig. 3. (a) A plot of 1/Sr and $^{87}Sr/^{86}Sr$ in the Jinsha River; (b) A plot of 1/Sr and Si/TZ$^+$ in the Jinsha River.
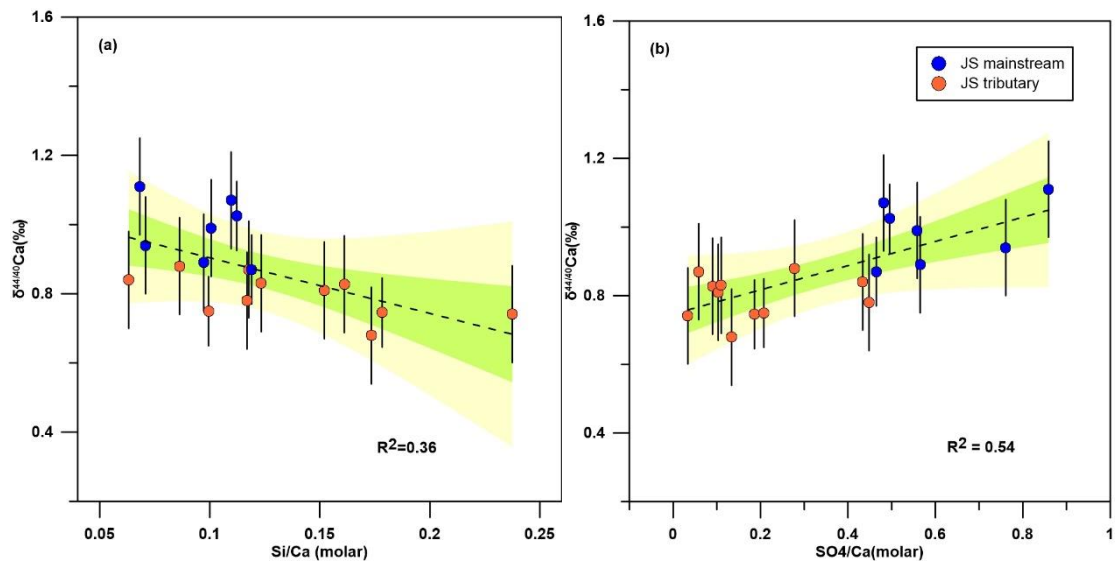
Fig. 4. (a) Plot of Si/Ca and $\delta^{44/40}Ca$ in the Jinsha River; (b) Plot of SO$_4$/Ca and $\delta^{44/40}Ca$ in the Jinsha River. The green and yellow areas represent 95% and 99.99% confidence interval, respectively.
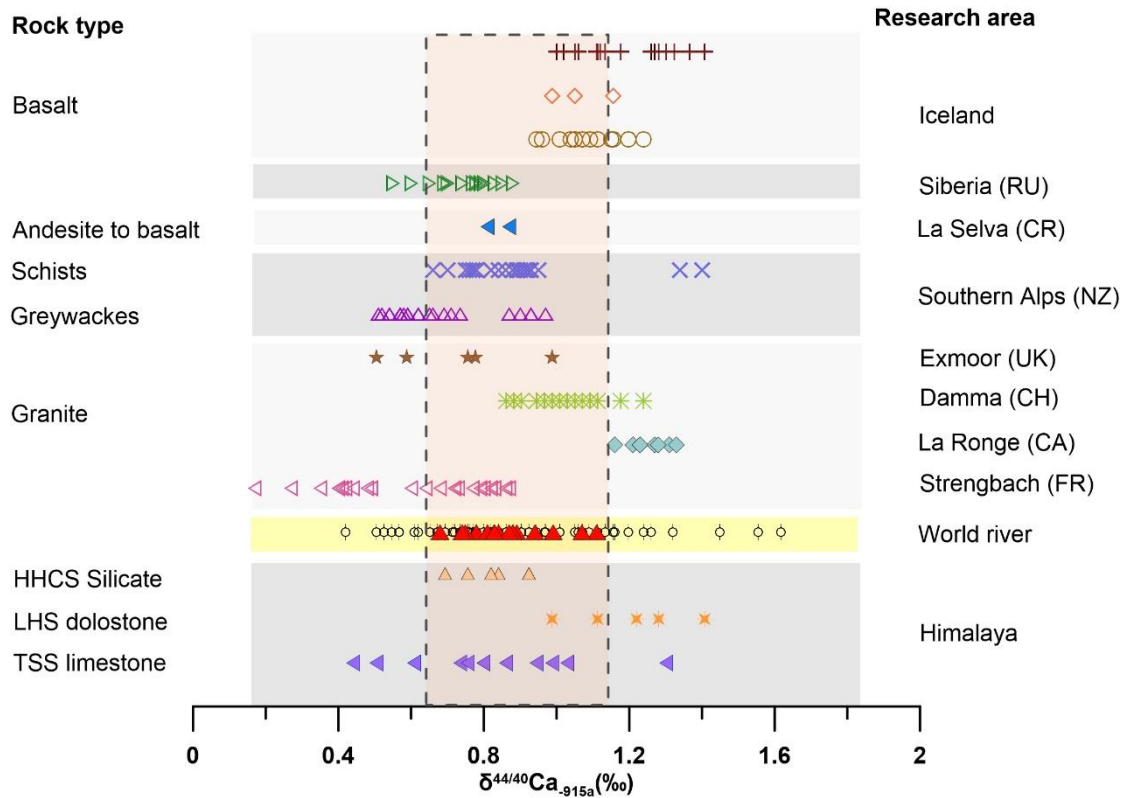
Fig. 5. Ca isotopic variation in river waters (modified from (Schmitt, 2016)). The red solid triangles represent our data in this study; world river data are from (Schmitt et al., 2003; Tipper et al., 2006; Tipper et al., 2010; Zhu and Macdougall, 1988) and other data sources can be seen in text. All values are normalized to the NIST SMR 915a standard.
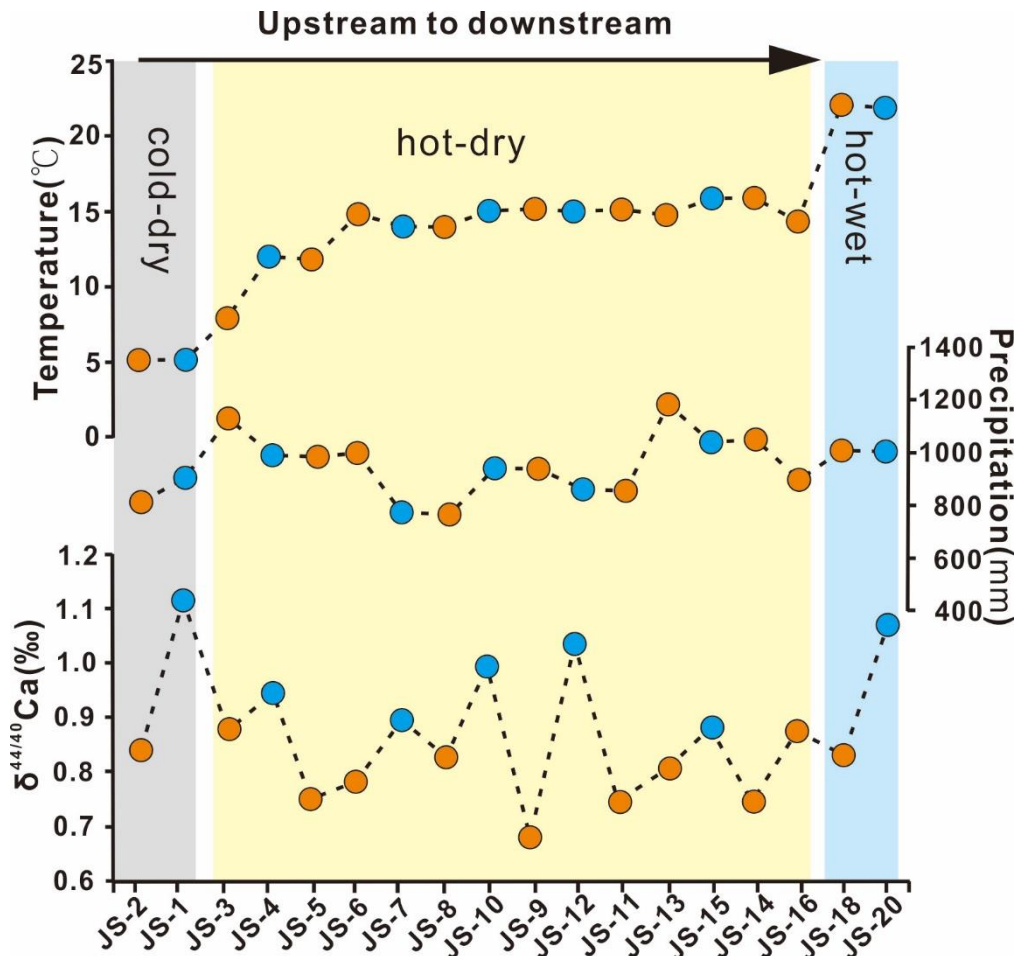
1134
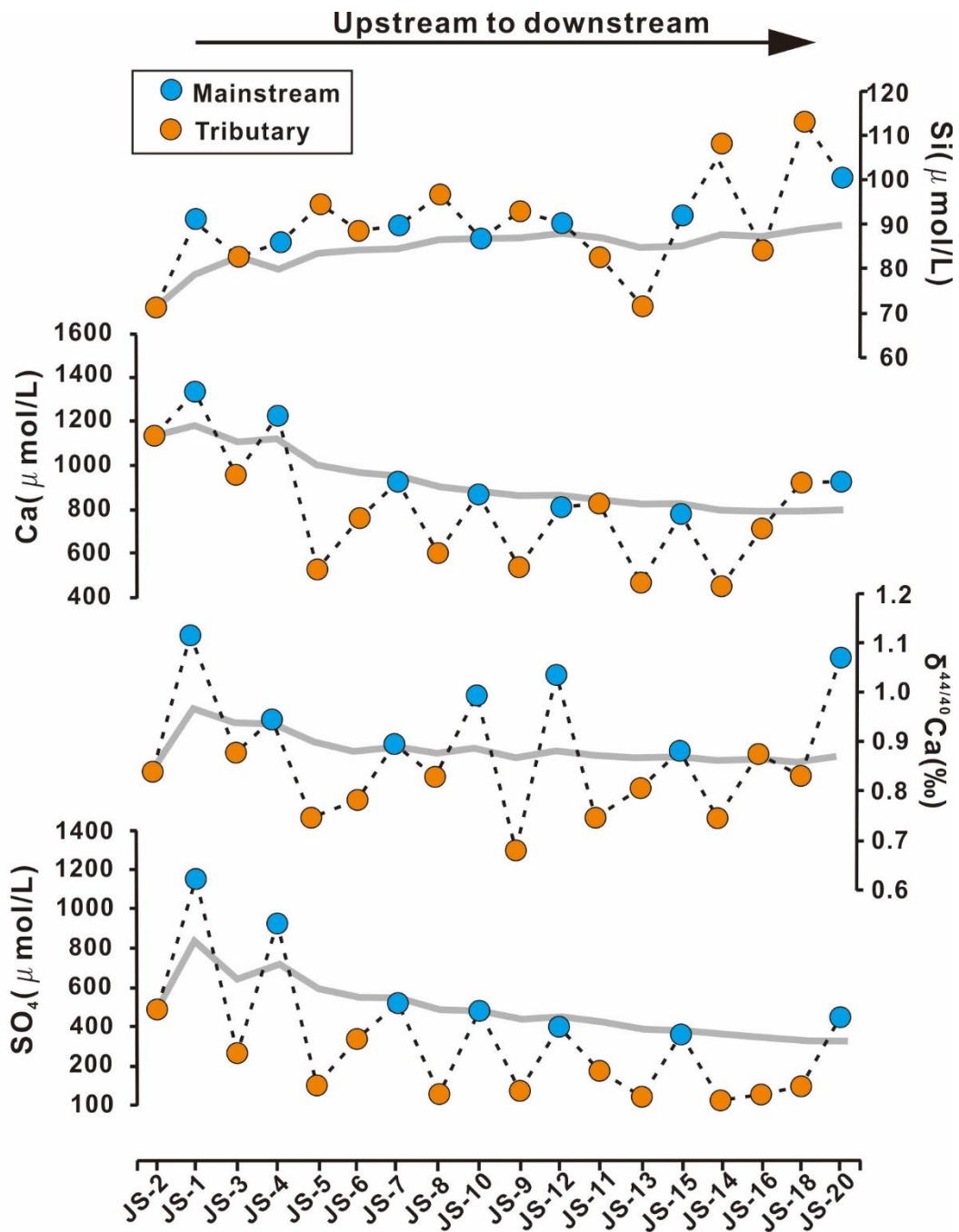
Fig. 6. Si, Ca and SO₄ concentrations and Ca isotope compositions of the

Jinsha River water samples from upstream to downstream. Grey lines

represent moving averages of all of the corresponding data.

1135

1136

1137

1138

Fig. 7. The change of climate factors (air temperature and precipitation) and Ca isotope compositions of the Jinsha River water samples from upstream to downstream. The Grey rectangle area represents the dry-cold climate, the yellow area represents the dry and hot environments and the blue area represents the hot-wet climate.
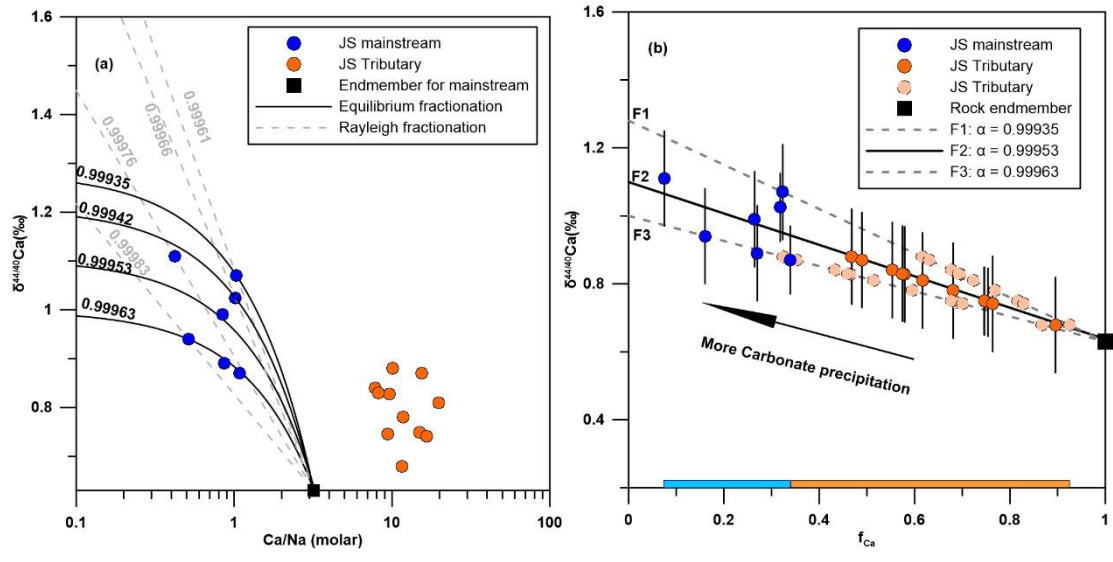
1146
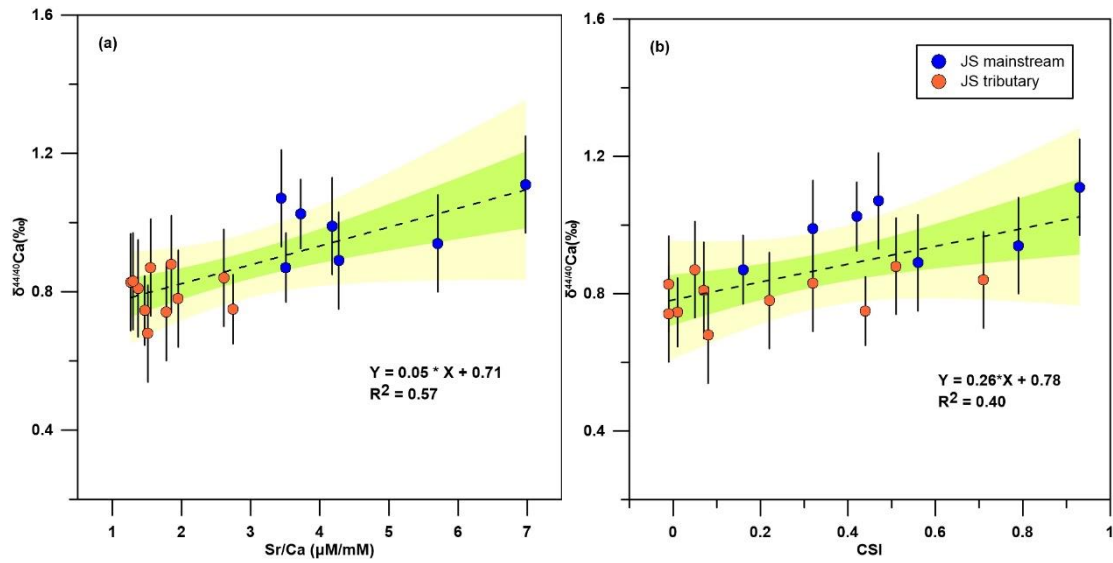
Fig. 8. (a) A plot of Sr/Ca and δ$^{44/40}$Ca in the Jinsha River; (b) A plot of CSI and

δ$^{44/40}$Ca in the Jinsha River. The green and yellow area represents the 95% and

99.99% confidence interval respectively.

1151

Fig. 9. The relationships between Ca isotope composition of river waters and

(a) dissolved Ca/Na ratios and (b) the fraction of Ca remaining in solution (f$_{Ca}$)

under the Equilibrium model.